Combining fugacity and physiologically based toxicokinetic concepts in a mechanistic model describing the fate of lipophilic contaminants in lactating cows ☆

Sylvain Lerch [a,b,*] , Olivier Martin [c] , Agnés Fournier [b], Isabelle Ortigues-Marty [d] , Jérôme Henri [e]

[a] *Ruminant Nutrition and Emissions, Agroscope, 1725 Posieux, Switzerland*
[b] *Université de Lorraine, INRAE, L2A, F-54000 Nancy, France*
[c] *Université Paris-Saclay, INRAE, AgroParisTech, UMR Modélisation Systémique Appliquée aux Ruminants, 91120 Palaiseau, France*
[d] *Université Clermont Auvergne, INRAE, Vetagro Sup, UMR Herbivores, 63122 Saint-Genès-Champanelle, France*
[e] *Fougères Laboratory, French Agency for Food, Environmental and Occupational Health and Safety (ANSES), 10B rue Claude Bourgelat, 35306 Fougères, France*

ARTICLE INFO

ABSTRACT

Quantifying the fate of lipophilic contaminants in lactating cows is the cornerstone for ensuring the chemical safety of dairy products and beef meat. Exploring the effects of cow feeding and physiology on the toxicokinetics of several lipophilic contaminants requires an integrative approach. This study developed and evaluated a mechanistic model (RuMoPOP) of the absorption, distribution, metabolism, and excretion (ADME) of lipophilic contaminant in lactating cows. The model's rationale relies on the coupling of ADME with physiological sub-models. The ADME sub-model merges the concepts and advantages of former fugacity and physiologically based toxicokinetic models. The physiological sub-model is based on a model that finely describes the dynamics of lipids in the digestive contents, body, and milk, depending on the milk production level (from a low-yielding suckler cow to a high-yielding dairy cow). The model was fitted to toxicokinetic data from two dairy cow experiments for polychlorinated biphenyls, dibenzo-*p*-dioxins, and dibenzofurans. Model performances for predicting milk accumulation and depuration kinetics were judged satisfactory, with an average root mean square error relative to the observed mean of 27%. The model makes it possible to predict the variability in accumulation and depuration kinetics, depending on contaminant lipophilicity, hepatic clearance rate, and diet lipid content and digestibility, over the whole lifespan of low- and high-yielding cows. The RuMoPOP model is a valuable tool for exploring the complex interplay between lipophilic contaminant properties and cow physiology and ultimately contributes to the chemical safety of diverse dairy and beef production systems towards legacy and emerging lipophilic contaminants.

1. Introduction

The chemical safety of animal-derived food products is a public health concern as well as a challenge for the long-term sustainability of livestock production systems (Hoogenboom et al., 2015; Weber et al., 2018). Persistent organic pollutants (POPs, e.g. polychlorinated biphenyls, PCBs; polychlorinated dibenzo-*p*-dioxins and dibenzofurans, PCDD/Fs) are lipophilic contaminants with chemical risks of concern in

animal products. These compounds are easily dispersed and highly persistent in the environment, and bioaccumulated in animal lipid-rich tissues (Zennegg, 2018). Thus, humans are chronically exposed to POPs mainly through the consumption of animal-derived food (90 % of the total PCDD/Fs and PCBs exposure; Malisch and Kotz, 2014), with ruminant milk and meat accounting for 35 % to 65 % of this exposure (BAG, 2013; EFSA, 2018). Although preventive measures have historically reduced emissions of some legacy POPs into the environment and bioaccumulation in animal feed and food chains (Hoogenboom et al., 2015), new threats linked to regulated or emerging contaminants constantly occur. Livestock production occasionally faces contamination incidents originating from accidentally contaminated feed or environmental pollution that compromise consumer's confidence, disrupt the agri-food chain economy, and induce social distress for farmers (Weber et al., 2018; Zennegg, 2018). Experiences gained from such incidents highlight how complex and challenging risk assessment and management are and how implications are of major concern (Hoogenboom et al., 2015).

Risk assessment of lipophilic contaminants requires quantifying their fate in the ruminant organism, which encompasses a series of toxicokinetic steps: absorption, distribution, metabolisation, and excretion (ADME). These processes are primarily investigated via feeding experiments under controlled conditions, from which transfer parameters (e.g. transfer rate, biotransfer and bioconcentration factors, and depuration half-life) are derived (Driesen et al., 2021; Driesen et al., 2022a). The investigations often focus on a single contaminant or a group of contaminants in a specific animal system, the latter considered a 'blackbox', where the specific ADME processes remain undeciphered (Amutova et al., 2021; Krause et al., 2023b). Such an empirical approach is time-consuming, costly, and fraught with ethical issues related to animal experimentation (i.e. number of animals used), often producing predictors that are hard to extrapolate to other circumstances, outside the specific context of the experiment (Klevenhusen et al., 2021). Indeed, even if precise and specific, such a methodology for risk assessment of contaminant transfer into farm animals is not generic, since transfer parameters depend both on the physicochemical properties of the contaminants and on animal feeding and physiology (Driesen et al., 2021; Driesen et al., 2022a; Lerch et al., 2024). These limitations are incompatible with the need for generic approaches that can reduce the need for animal testing. A more comprehensive and systematic approach can fill these gaps by developing dynamic and multicompartmental toxicokinetic models (Armitage et al., 2021; Klevenhusen et al., 2021; Lautz et al., 2019; Moenning et al., 2023b). Toxicokinetic models describe the ADME processes of a contaminant in an animal organism and allow extrapolation beyond the framework of preexisting in vivo experimental data. For researchers, conceptualising and developing toxicokinetic models provide a medium for the long-term integration of dispersed knowledge and a tool for testing research hypotheses. For risk assessors and managers, toxicokinetic models enable the exploration of complex scenarios of contaminant exposure and depuration and help in decision making or identifying relevant scenarios to test in vivo.

A few multi-compartmental toxicokinetic models describing the ADME of lipophilic contaminants in lactating cows have been developed so far. They follow two types of formalism: the fugacity concept (Mackay, 2001) or the physiologically based toxicokinetic (PBTK) principle (Moenning et al., 2023b). A cow fugacity model was initially developed by McLachlan (1994), with further developments and uses by Rosenbaum et al. (2009), Tremolada et al. (2014), and Takaki et al. (2015). Three compartments—the digestive tract, blood, and fat—are represented with advective, diffusive, and degradation fluxes at the interfaces (McLachlan, 1994). The main interest of this model is the representation of reversible diffusive fluxes in series across lipid and water layers at the interfaces of digestive tract to blood and of blood to fat. Such fluxes are governed by the contaminant partition coefficient between octanol and water (K_{ow}) and adequately reproduce biological

observations (Kelly et al., 2004; McLachlan, 1994). Nevertheless, the specific McLachlan (1994) model have limitations: (i) a static description of cow feeding and physiology (i.e. the volumes of the three compartments are defined initially only and do not evolve dynamically over time); (ii) a weak representation of body distribution, with only blood and fat compartments; and (iii) consequently, a lack of separate estimates of the metabolic clearance of the contaminant by the liver, as this specific organ is not represented alone (McLachlan, 1994). In human, some of those limitations were tackled along the development of a more complex model for lipophilic contaminants based on the fugacity concept (Cahill et al., 2003). As far as the authors are aware of, these additional developments were not address so far for the cow fugacity model of McLachlan (1994). Two cow PBTK models for lipophilic contaminants were initially developed by Derks et al. (1994) and MacLachlan (2009) and were further extended by Bogdal et al. (2017) and Moenning et al. (2023a); Moenning et al. (2023c). The main advantages of existing PBTK models encompass body distribution that varies according to the volume and blood perfusion rate of the corresponding tissue or organ, as well as the separate liver and udder representations, which allows deciphering the respective routes of contaminant elimination through hepatic metabolism and milk excretion. Their main limitations include (i) a weak representation of the absorption and faecal excretion processes (i.e. the digestive tract compartment is not represented), and ii) a limited flexibility and genericity in the description of the kinetics in volume and blood irrigation of body compartments in relation to the lactation cycle. These limitations in pre-existing cow fugacity and PBTK models for lipophilic contaminants reduce their genericity and preclude their routine use.

The aim of the present study was to develop, adjust, and evaluate a mechanistic and dynamic model that describes the toxicokinetic of lipophilic contaminants from oral intake up to accumulation in the body and secretion in the conceptus and milk of dairy and suckler beef cows
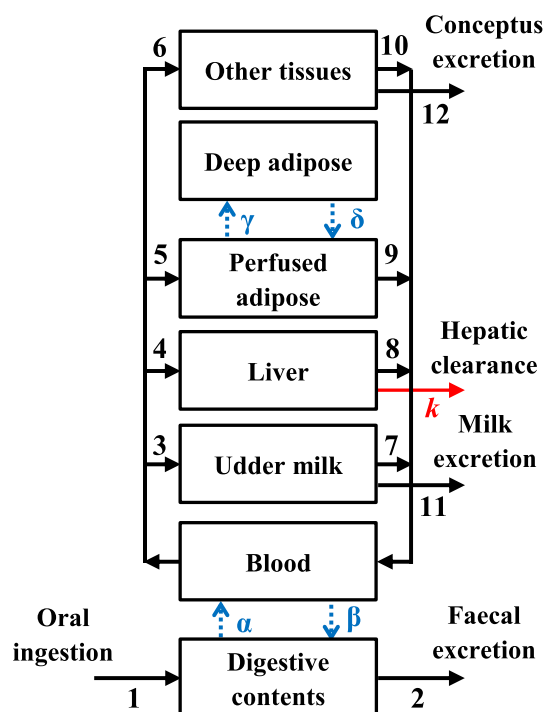
Fig. 1. Forester diagram of the RuMoPOP physiologically based toxicokinetic (PBTK) model describing the fate of lipophilic contaminants into lactating cow in function of its lipid digestion and physiology. According to the fugacity concept, solid thin black lines represent advective fluxes, dotted blue lines represent passive diffusion fluxes, and the solid thick red line represents transformation (hepatic metabolism) flux. Conceptus encompasses foetus, placenta and foetal fluids excreted once yearly at calving.

Table 1

Main parameters and variables of the absorption, distribution, metabolism, and excretion (ADME) of lipophilic contaminant sub-model, and the physiological (including ingestion and digestion) sub-model of lactating cow.[1]

Item	Acronym	Unit	Description
ADME fluxes			
Advection (Equation [1])			
Oral intake and faecal excretion (arrows 1 and 2 in Figure 1)			
	$Q^2_{feed\&soil \to digestive\ contents}$	kg DM day^{-1}	Oral feed and soil dry matter intake
	$Q_{digestive\ contents \to faeces}^2$	kg lipids h^{-1}	Faecal lipid excretion
Blood-tissues distribution (arrows 3 to 10 in Figure 1)			
	$Q^3_{blood/udder}$	kg h^{-1}	Blood perfusion to the udder
	$Q^3_{blood/liver}$	kg h^{-1}	Blood perfusion to the liver
	$Q^3_{blood/adipose\ tissues}$	kg h^{-1}	Blood perfusion to the adipose tissues
	$Q^3_{blood/other\ tissues}$	kg h^{-1}	Blood perfusion to the other tissues
	P^4_{udder}	unitless	Partition coefficient between blood and udder
	P^5_{liver}	unitless	Partition coefficient between blood and liver
	$P^5_{adipose\ tissues}$	unitless	Partition coefficient between blood and adipose tissues
	$P^6_{other\ tissues}$	unitless	Partition coefficient between blood and other tissues
	$Cont\ Corr\ P^6_{udder}$	unitless	Corrective factor for blood to udder (milk lipid) partition coefficient (P_{udder}) for single contaminant
Milk excretion (arrow 11 in Figure 1)			
	$Q^2_{udder \to milk\ Lip}$	kg lipids day^{-1}	Milk lipid excretion (discrete event at each milking or suckling)
Conceptus excretion (arrow 12 in Figure 1)			
	$Q_{other\ tissues \to conceptus}^2$	kg lipids year^{-1}	Conceptus (foetus, placenta and foetal fluids) lipid excretion at calving (yearly discrete event)
Diffusion (Equation [4])			
Contaminant lipophilicity			
	$Cont\ K^7_{ow}$	unitless	Partition coefficient between octanol and water
Absorption & non-biliary excretion (arrows α and β in Figure 1)			
	$Q^8_{Wat\_digestive\ contents/blood}$	kg day^{-1}	Diffusive parameter across the water layer at the intestine/blood interface
	$Q^8_{Lip\_digestive\ contents/blood}$	kg day^{-1}	Diffusive parameter across the lipid layer at the intestine/blood interface
Perfused-deep adipose tissues distribution (arrows δ and γ in Figure 1)			
	$Q^8_{Wat\_perfused/deep\ adipose}$	kg day^{-1}	Diffusive parameter across the water layer at the perfused/deep adipose tissues interface
	$Q^8_{Lip\_perfused/deep\ adipose}$	kg day^{-1}	Diffusive parameter across the lipid layer at the perfused/deep adipose tissues interface
Degradation (Equation [5])			
Hepatic metabolism (arrow *k* in Figure 1)			
	$Cont\ k^9_{met}$	day^{-1}	Metabolic first-order clearance rate in the liver
Physiological traits			
Lactating cow productivity			
	POT	10 kg day^{-1}	Raw milk yield at the peak of lactation[10]
Ingestion and digestion[11]			
	Intake DM content	kg DM kg^{-1}	Intake dry matter content
	Intake lipid content	kg kg^{-1} DM	Intake lipid content
	Intake Non-Lip OM content	kg kg^{-1} DM	Intake non-lipid organic matter content
	Intake ash content	kg kg^{-1} DM	Intake ash content
	Dig lipids	kg kg^{-1}	Lipid digestibility
	Dig Non-Lip OM	kg kg^{-1}	Non-lipid organic matter digestibility
	Dig ashes	kg kg^{-1}	Ash digestibility
	Digestive contents FM	kg	Digestive content total mass
	Digestive contents water content	kg water kg^{-1}	Digestive contents water content
	Digestive contents lipid content	kg lipids kg^{-1}	Digestive contents lipid content
	Digestive contents lipids	kg	Digestive contents lipid mass
	$Q_{FM\ faeces}$	kg h^{-1}	Faecal fresh matter excretion
Milk production[12]			
	Q_{RMY}	kg day^{-1}	Raw milk yield
	Milk lipid content	kg kg^{-1}	Milk lipid content
Body weight and composition			
	BW	kg	Body weight
	EBW	kg	Empty body weight
	Lip EB	kg	Empty body lipid mass
	Wat EB	kg	Empty body water mass
	Prot EB	kg	Empty body protein mass
	Ash EB	kg	Empty body ash mass
	FM i	kg	Total mass of the body compartment *i*[13]
	Lip i	kg	Lipid mass of the body compartment *i*[13]

[1]Calculations of parameter and variable values are reported in the main text and Supplementary Information S1-S7, whereas typical ranges are illustrated in Table 2, Supplementary Table S1 and Supplementary Fig. S1.

[2]Physiological traits (i.e. feed and soil intake and digestibility, milk yield and lipid content, body weight and lipid content) are described thanks to coupling to the cow digestion and physiological sub-model of Martin and Sauvant (2007) for cow producing between 10 and 50 kg of milk per day at the peak of lactation. These are additionally illustrated in Supplementary Fig. S1.

[3]Values for blood perfusion rates of tissues are gathered from MacLachlan (2009) and multiplied by tissue mass, except for udder blood perfusion that depends on raw milk yield, and liver blood perfusion that depends on body weight and dry matter intake according to Lescoat et al. (1996).

[4]Udder compartment is considered equal to the milk lipid excreted twice daily. Therefore, the blood-to-udder partition coefficient P_{udder} is fixed to the milk-blood ratio of lipid concentrations, which is further corrected by the *Cont Corr P_{udder}* factor.

[5]Blood-to-tissue partition coefficients are fixed to the tissue-blood ratio of total lipid concentrations, assuming that non-polar lipophilic contaminants would diffuse almost exclusively into lipids (MacLachlan, 2009).

[6]A corrective factor of the blood-to-udder partition coefficient that depends on the *Cont K_{ow}* of single lipophilic contaminant congener is applied to account for the curvilinear decrease in observed partition coefficient as a function of the log *Cont K_{ow}* (see Supplementary Information S2 for details).

over successive gestation and lactation cycles. The hypothesis was that the simultaneous, fine, and mechanistic description of the ADME and cow physiology and feeding allows the exploration of the complex interplay between divergent contaminant properties (lipophilicity and metabolic susceptibility), the lactating cow physiology (milk production level and concomitant pattern in body lipid dynamic), and diet composition (lipid content and digestibility).

2. Material and methods

2.1. Model description

2.1.1. Rationale and overview

The proposed model, which we called RuMoPOP, describes the fate of lipophilic contaminants (e.g. POPs) in the lactating cow. It consists of two connected sub-models: (i) an ADME sub-model describing the contaminant ingestion and toxicokinetic; and (ii) a physiological sub-model describing the dynamics of lipids in the digestive contents, empty body (full body minus digestive contents, urine, and conceptus), conceptus, and milk over the gestation and lactation cycle. For the development of the ADME sub-model, the rationale was to combine mechanistic formalisms of contaminant advective, diffusive, and transformation fluxes previously described in pre-existing fugacity (McLachlan, 1994) and PBTK (Derks et al., 1994; MacLachlan, 2009) models. Specific developments were targeted at selecting and coupling the respective advantages of the former fugacity and PBTK formalisms, equations, and parameters in the ADME sub-model. The development of the physiological sub-model took advantage of Martin and Sauvant (2007) mechanistic model, which finely describes the lactating cow metabolism associated with productive performance (especially intake, milk, and body lipid dynamics) depending on the milk production potential of low-yielding suckler cows up to high-yielding dairy cows. Additional developments allowed a fine description of digestive processes and of conceptus growth and parturition along gestation, whereas the compartmentation of the physiological sub-model was adapted to match that of the ADME sub-model (i.e. allocation of body total and lipid masses of the physiological sub-model into the specific tissues and organs represented in the ADME sub-model). The conceptual diagram of the ADME sub-model is presented in Fig. 1, and the main parameters are listed in Table 1. The detailed features of the model are described below.

2.1.2. Sub-model of lipophilic contaminant ADME

The ADME sub-model describes the time-dependent kinetics of lipophilic contaminant amounts (ng) from oral intake ($Q_{feed\&soil \to digestive\ contents}$) into seven digestive and body compartments and four elimination routes (Fig. 1). A lipophilic contaminant enters the system by oral intake to the *Digestive contents* compartment, where it may be absorbed into the *Blood* and subsequently distributed to tissue and organ compartments (*Perfused* and *Deep adipose tissues*, *Liver*, *Udder milk* and *Other tissues*). *Udder milk* is considered to amount to half of the daily milk yield (Q_{RMY}, assuming a 0.5 d interval between milking, representing the case of a twice-daily milking dairy cow, with 12 h between each milking),

whereas *Other tissues* represent the rest of the body (i.e. full body minus *Digestive contents, Blood, Perfused* and *Deep adipose tissues*, and *Liver*), including the *Conceptus* (i.e. the sum of foetus, placenta, and fluids). The lipophilic contaminant may be eliminated from the system through *Faecal, Milk* (at milking or suckling), and *Conceptus* (at parturition) excretion routes or by liver metabolism (*Hepatic clearance*; Fig. 1). To represent all the contaminant inter-compartmental fluxes, three types of processes were used: advection (black arrows 1 to 12 in Fig. 1), diffusion (dotted blue arrows α to γ), or transformation (red arrow k) (Mackay, 2001).

2.1.2.1. Advection fluxes.
Advective transport processes are unidirectional fluxes in which lipophilic contaminants are transferred from one compartment to another together with an advective medium (12 black arrow numbers 1 to 12 in Fig. 1; Mackay, 2001). Advective fluxes are defined as the product of the contaminant concentration in the advective medium (i.e. diet, faeces, blood, milk, or conceptus) with the rate of transit of the given medium from compartment i to j ($Q_{i \to j}$), as defined in Equation (1):

$$Adv.\ Cont_{i \to j}\ (\text{ng day}^{-1}) = \left[A_i\ (\text{ng})\ /\ M_i\ (\text{kg}) \right]\ \times\ Q_{i \to j}\ (\text{kg day}^{-1})\ \left[\times\ 1\ /\ P_i\ (\text{unitless}) \right] \tag{1}$$

where A_i is the contaminant amount in the leaving compartment i and M_i its mass, and $Q_{i \to j}$ is one of the following: the rate of oral intake ($Q_{feed\&soil \to digestive\ contents}$, arrow number 1), faecal excretion ($Q_{digestive\ contents \to faeces}$, arrow number 2), blood perfusion to (arrow numbers 3 to 6), or back from (arrow numbers 7 to 10), the four body tissues for distribution ($Q_{blood/udder}$, $Q_{blood/liver}$, $Q_{blood/adipose\ tissues}$, and $Q_{blood/other\ tissues}$), milk excretion ($Q_{udder \to milk}$, arrow number 11), or conceptus excretion ($Q_{other\ tissues \to conceptus}$, a yearly discrete event at calving, arrow number 12; Table 1 and Fig. 1). The partition coefficient P_i reflects the *Tissue$_i$* − *Blood* ratio of the contaminant concentrations at equilibrium and is only included for the four fluxes back to *Blood* from *Udder, Liver, Perfused adipose*, and *Other tissues* compartments (arrow numbers 7 to 10).

In the case of blood distribution, Equation (1) also corresponds to the "blood perfusion-limited flux" formalism used in most PBTK models (Bogdal et al., 2017; Derks et al., 1994; MacLachlan, 2009; Moenning et al., 2023a; Moenning et al., 2023c). The daily blood perfusion rates ($Q_{blood/tissue\ i}$) to each of the four tissues were fitted as described in Supplementary Information S1. The partition coefficient (P_i) for *Liver, Perfused adipose tissues*, and *Other tissues* was assumed to be equal to the ratio of total lipid concentrations (%fresh weight) in *Tissue i* to that in *Blood* (MacLachlan, 2009). Such a generic and mechanistic way to set P_i was retained because highly lipophilic (i.e. characterised by a $K_{ow} \geq 10^3$) and apolar contaminants diffuse almost exclusively into total lipids, and thus, at equilibrium, contaminant concentrations normalised to lipid weight are assumed to be equal in *Blood* and any *Tissues*. A similar calculation was performed for P_{udder}, with a further adjustment to

account for the lipophilicity degree of the contaminant (*Cont K_{ow}*):

1994). As successive diffusive transports across water and lipid phases occur in series, the sum of each single reciprocal diffusive transport

$$P_{udder} \text{ (unitless)} = [\text{Milk lipid content (\% fresh weight)} / \text{Blood lipid content (\% fresh weight)}] \times \text{Cont Corr } P_{udder} \text{ (unitless)} \qquad (2)$$

with *Cont Corr P_{udder}* being equal to:

$$\text{Cont Corr } P_{udder} \text{ (unitless)} = \left(1.03 \times log_{10} \text{ Cont } K_{ow}^{-21.04}\right) / \left(7.67^{-21.04} + log_{10} \text{ Cont } K_{ow}^{-21.04}\right) \qquad (3)$$

value gives the total resistance to lipophilic contaminant transport (Mackay, 2001), as defined in Equation (4):

$$\text{Diff. Cont}_{i \rightarrow j} \text{ (ng day}^{-1}) = [A_i \text{ (ng)} / M_i \text{ (kg lipids)}] / [(1 / Q_{Lip\_i/j} \text{ (kg day}^{-1})) + (\text{Cont } K_{ow} \text{ (unitless)} / Q_{Wat\_i/j} \text{ (kg day}^{-1}))] \qquad (4)$$

Full details about the fitting of the corrective factor *Cont Corr P_{udder}* to *Cont K_{ow}* are provided in Supplementary Information S2.

Lipophilic contaminant excretion is represented as a continuous flux for the faecal route (i.e. from the *Digestive contents* compartment at a constant faecal excretion rate $Q_{digestive\ contents \rightarrow faeces}$). In case of the milk excretion route, it is represented as discrete events (e.g. for twice daily milking: twice per day, at 0.5 day interval, the *Udder Milk* is emptied from contaminant), as for the conceptus excretion route (i.e. yearly calving event: the amount of contaminant distributed into the lipid mass of conceptus is excreted out of the *Other tissues* compartment).

2.1.2.2. Diffusion fluxes. According to the fugacity concept, diffusive transports are reversible fluxes in which lipophilic contaminants cross the phase between two compartments by passive diffusion along their concentration gradients (four dotted blue arrows α, β, γ and δ in Fig. 1; Mackay, 2001). They are calculated as the product of a diffusive parameter that characterises the phase to cross ($Q_{i/j}$, i.e. water- or lipid-rich phases) with the contaminant concentration in it (Mackay, 2001). Reversible diffusive fluxes are implemented at the *Digestive contents/ Blood* interface to represent both absorption (arrow α) and reverse non-biliary secretion across the intestinal wall (arrow β) along the concentration gradient of lipophilic contaminants between *Digestive contents* and *Blood* lipids. Indeed, lipophilic and apolar contaminants excreted as parent compounds from the body to the faeces originate almost exclusively from such a passive diffusion process across the intestinal wall, rather than from biliary excretion or exfoliation of intestinal enterocytes (Jandacek and Tso, 2001; Rozman, 1986).

Additional reversible diffusive fluxes are implemented at the *Perfused adipose/Deep adipose* interface (arrows γ and δ) to represent the late (re) distribution pattern of lipophilic contaminants to adipose tissues (McLachlan, 1994; Richter and McLachlan, 2001; Wiener et al., 1976). In such cases, the *Perfused adipose* compartment represents the adipocyte extra-cellular matrix, membrane, and cytosol (fitted to 5 % of the total *Adipose tissues* weight), whereas the *Deep adipose* represents the adipocyte triglyceride-rich vacuoles (fitted to 95 % of the total *Adipose tissues*; Mariman and Wang, 2010; Vernon, 1980).

For both *Digestive contents/Blood* and *Perfused adipose/Deep adipose* interfaces, the total diffusive transport includes the lipophilic contaminant crossing of a lipid phase and of a water phase in series. For the *Digestive contents/Blood* crossing, the water phase represents the unstirred water layer surrounding the microvilli of the intestinal wall, and the lipid phase considers the lipid bilayer of the enterocyte membrane (Kelly et al., 2004). In the case of the *Perfused adipose/Deep adipose* crossing, the lipid phase represents the lipid bilayer of the adipocyte membrane, and the water phase represents the adipocyte cytosol (McLachlan,

where $Q_{Lip\_i/j}$ and $Q_{Wat\_i/j}$ are the diffusive parameters between compartments i and j of the lipid and water phases, respectively, corresponding to either the *Digestive contents/Blood* or *Perfused adipose/Deep adipose* interface. The lipophilic contaminant concentration (A_i/M_i) is expressed on a lipid weight basis, whereas the *Cont K_{ow}* term for the water phase diffusion step is used to convert the specific contaminant lipid-normalised concentration into a water-normalised one (assuming that the lipid-normalised concentration equals the octanol-normalised one). At the *Perfused adipose/Deep adipose* interface, we used the diffusive parameters of the cow fugacity model of McLachlan (1994), that is, 4.264 and 14,137,620 kg day^{-1} for $Q_{Lip\_perfused/deep\ adipose}$ and $Q_{Wat\_perfused/deep\ adipose}$, respectively. At the *Digestive contents/Blood* interface, we re-evaluated $Q_{Lip\_digestive\ contents/blood}$ and $Q_{Wat\_digestive\ contents/blood}$ as 0.5002 and 3,479,260 kg day^{-1}, considering estimations of the dietary lipid content and digestibility in the specific cow PCB and PCDD/F toxicokinetic study (McLachlan, 1993) that were used for the initial calibration of the McLachlan (1994) model (see Supplementary Information S3 for details). Such a mechanistic view of the diffusive transfer into the water phase implies that when *Cont K_{ow}* increases, the diffusive transfer rate decreases. This inverse relationship between diffusion transfer rate and *Cont K_{ow}* is consistent with biological observations that established a quantitative link between contaminant lipophilicity and its absorption rate (Kelly et al., 2004; McLachlan, 1994), as well as the delay in equilibrium of distribution between blood and adipose tissues (Rey-Cadilhac et al., 2020; Richter and McLachlan, 2001).

2.1.2.3. Transformation flux. The liver is considered to be the sole site for lipophilic contaminant elimination through transformation (i.e. metabolic clearance, single red arrow *k* in Fig. 1), a process described according to a metabolic first-order rate (MacLachlan, 2009), as defined in Equation (5):

$$\text{Trans. Cont}_{Liver} \text{ (ng day}^{-1}) = A_{Liver} \text{ (ng)} \times \text{Cont } k_{met} \text{ (day}^{-1}) \qquad (5)$$

where, A_{Liver} is the amount of lipophilic contaminant in the *Liver* compartment, and *Cont k_{met}* is the metabolic first-order clearance rate of the specific contaminant. The *Cont k_{met}* parameter was fitted for PCB and PCDD/F congeners as outlined in Section 2.2. Assumption of a linear rate of biotransformation of lipophilic contaminants proportional to amounts in the liver is realistic, considering that model simulations are mainly performed for usual and moderate ranges of contaminant concentrations in the diet and body that are encountered on-field. These concentration ranges are usually far from the ones implying hepatic metabolism induction or saturation (Cahill et al., 2003).

Table 2
Polychlorinated biphenyl (PCB) and dibenzo-*p*-dioxin and dibenzofuran (PCDD/F) congener-specific parameters, and dosing or diet concentration representing the toxicokinetic experiments used for fitting the metabolic first-order clearance rate in the liver (k_{met}) of the lactating cow RuMoPOP model.

Congener	Literature log K_{ow}[1]	Fitted k_{met} (d^{-1})[2]	Contaminant dosing (ng d^{-1}) or diet concentration (ng kg^{-1} dry matter)[3] in the toxicokinetic study for fitting of k_{met}[4]	
			Lorenzi et al. (2020)	Huwe and Smith (2005)
iPCBs				
28	5.6	2937	30,720	
52	5.8	394	30,248	
101	6.3	110	28,512	
138	6.7	2.0	13,863	
153	6.8	2.0	30,733	
180	7.2	2.9	30,248	
dlPCBs				
77	6.4	23.0	140	
126	7.0	2.2	140	*0.759/0.18*
169	7.5	0.5	140	*0.501/0.045*
81	6.4	17.4	140	
105	6.6	0.5	140	
114	6.6	3.0	140	
118	6.7	0.0	140	
123	6.7	4.0	140	
156	7.1	0.5	140	
157	7.1	2.4	140	
167	7.2	0.5	140	
189	7.6	0.0	140	
PCDDs				
2,3,7,8-TCDD	6.6	3.0	0.553	
1,2,3,7,8-PeCDD	7.2	1.7	*2.76*	0.363/0.066
1,2,3,4,7,8-HxCDD	7.6	0.6	*2.76*	1.134/0.029
1,2,3,6,7,8-HxCDD	7.6	0.3	*2.76*	1.661/0.111
1,2,3,7,8,9-HxCDD	7.6	1.4	*2.76*	1.345/0.064
1,2,3,4,6,7,8-HpCDD	8.0	1.7	*2.76*	22.863/1.212
OCDD	8.4	4.3	*5.52*	59.635/6.357
PCDFs				
2,3,7,8-TCDF	6.5	40.0	0.553	
1,2,3,7,8-PeCDF	7.0	61.0	*2.76*	1.159/0.049
2,3,4,7,8-PeCDF	7.1	2.0	*2.76*	2.391/0.08
1,2,3,4,7,8-HxCDF	7.5	0.8	*2.76*	8.04/0.102
1,2,3,6,7,8-HxCDF	7.6	0.8	*2.76*	6.093/0.062
1,2,3,7,8,9-HxCDF	7.7	12.0	2.76	
2,3,4,6,7,8-HxCDF	7.6	1.0	*2.76*	8.664/0.048
1,2,3,4,6,7,8-HpCDF	8.0	2.5	*2.76*	59.8/0.211
1,2,3,4,7,8,9-HpCDF	8.2	0.8	*2.76*	7.742/0.018
OCDF	8.6	3.1	*5.52*	50.749/0.315

Abbreviations: indicator polychlorinated biphenyls (iPCBs), dioxin-like polychlorinated biphenyls (dlPCBs), polychlorinated dibenzo-*p*-dioxins (PCDDs), polychlorinated dibenzofurans (PCDFs), decimal logarithm of the partition coefficient between octanol and water (log K_{ow}), Metabolic first-order clearance rate in the liver (k_{met}).

[1] Gather from Amutova et al. (2021).

[2] For all PCB congeners, as well as 2,3,7,8-TCDD, 2,3,7,8-TCDF, and 1,2,3,7,8,9-HxCDF, the dataset of Lorenzi et al.'s (2020) study was used for calibration, and for all the others 14 PCDD/F congeners, the dataset of the Huwe and Smith (2005) study was used for calibration of the k_{met} parameter.

[3] Daily dosing through spiked oil during the exposure period is reported for Lorenzi et al.'s (2020) study, whereas contaminated diet concentrations during the 40-days exposure followed by 40-days depuration are reported in the respective order separated by a dash for the Huwe and Smith (2005) study. Data in italics are for the study that served for evaluation for the respective congener.

[4] Simulation time frame corresponding to the experimental designs of the dairy cow toxicokinetic experiments that serve for fitting of k_{met}: Lorenzi et al. (2020), 49 days exposure follow by 42 days depuration, from 115 to 206 days in milk; Huwe and Smith (2005): 40 days exposure follow by 40 days depuration, from 191 to 271 days in milk.

2.1.3. Sub-model of lactating cow physiology

Resolving the differential equations of the ADME sub-model and computing the lipophilic contaminant fluxes, masses, and concentrations require the kinetics in total and lipid masses of oral intake, digestive contents, body tissue compartments, faeces, milk, and conceptus. These parameters were obtained from the physiological sub-model developed from Martin and Sauvant's (2007) mechanistic model of lactating cow metabolism. This model offers a useful platform for the fine-tuned and realistic description of the kinetics of feed intake, and milk production and composition. It also finely describes changes in body weight (BW) and composition (including lipids) during a lactation cycle of 300 days. One of the major advantages of this model is its ability to behave reliably when milk yield potential (*POT* parameter in Table 1) varies from 10 to 50 kg day^{-1} at the lactation peak, which allows for the description of both suckler beef and dairy cows. Supplementary Fig. S1 illustrates the kinetics in such key traits described by the physiological sub-model for *POT* of 10 (2,000 kg per lactation of 300 days: low-yielding suckler beef cow) and 50 kg day^{-1} at the lactation peak (12,000 kg per lactation: high-yielding dairy cow). Additional variables gathered from the physiological sub-model are listed in Table 1. Full details about the model framework and equations are described in Martin and Sauvant (2007).

In an attempt to couple the physiological sub-model with the ADME sub-model, the body compartmentation represented in the original Martin and Sauvant (2007) model was adjusted to fit the specific tissue compartments represented in the ADME sub-model. This especially implied the allocation of the empty body total lipid mass (*Lip EB*) to the *Adipose tissues* and *Other tissues* compartments. This was ensured by fitting allometric relationships based on 234 cow's body dissections and chemical analyses gathered from the slaughterhouse database of INRAE

(see details in Supplementary Information S4). Moreover, the total lipid concentration kinetics of the blood were derived from a compilation of experimental data (see details in Supplementary Information S5).

Some additional developments were included to represent digestion and gestation that were not initially included in the Martin and Sauvant (2007) model. The kinetics in total and lipid masses of the *Digestive contents* compartment and *Faeces* excretion required the use of part of the teleonomic cow model of Martin and Sauvant (2010a,b), together with specific dietary nutrient contents and digestibility, that should be set by the user depending on the specific diet fed to the cow. These parameters are listed in Table 1, and details of this additional development are provided in Supplementary Information S6. The kinetics in total and lipid mass of the *Conceptus* were introduced along a gestation of 286 days thanks to the allometric equations of foetus, placenta, and fluids of Ferrell et al. (1976). Gestation starts 79 days after calving (time of conception) and ends 365 days later (calving-to-calving interval of one year). As lactation length is set to 300 days, a prepartum dry-off period is included to cover a year (see details in Supplementary Information S7). This allows running the model over repeated reproductive cycles throughout the lifespan of the lactating cow, simulating its consequences on the lipophilic contaminant toxicokinetic.

2.1.4. Model implementation

The model was implemented using the software Vensim® Professional version 9.3.2 (Ventana Systems, Inc.), and the corresponding file and code are provided in a data repository available online at Doi: 10.5281/zenodo.14218322. Numerical integration of differential equations was completed with the Runge-Kutta 4 method, with a fixed step of integration of $1/128 = 7.8125 \times 10^{-3}$ h, which corresponds to a 0.47-min interval, and simulations can be run over 10 successive gestation-lactation cycles.

2.2. Model fitting and evaluation of predictive capabilities for PCBs and PCDD/Fs

Using the RuMoPOP model to simulate the toxicokinetic of a lipophilic contaminant requires setting 11 input parameters. These include eight parameters of the physiological sub-model characterising lactating cow productivity (*POT*) and diet composition (contents and digestibility of dry matter, lipids, non-lipid organic matter and ash), which are determined for each situation studied using, for instance, feed nutritive values from the literature (e.g. INRA et al., 2018). The contaminant concentration of the diet must be defined, and it is also case-dependent. The two remaining input parameters of the ADME sub-model are characteristics of the lipophilic contaminant under study: its lipophilicity (*Cont K_{ow}*) and metabolic clearance rate (*Cont k_{met}*). A range of *Cont K_{ow}* estimates is easily available from the literature for almost every lipophilic contaminant of interest (e.g. Mackay et al., 2006). Conversely, *Cont k_{met}* has to be calibrated for every contaminant.

In the present investigation, *Cont k_{met}* values were fitted for the six indicator PCBs (iPCBs), 12 dioxin-like PCBs (dlPCBs), and 17 2,3,7,8-chloro-substituted PCDD/Fs, all currently regulated in feed (Regulation EU n°277/2012) and food of animal origin (Regulation EU n°1259/2011). For every single congener, *Cont k_{met}* value was adjusted using the Payoff procedure of Vensim® (v. 9.3.2), that intend to shorten the sum of squares error between the milk concentrations from model simulations and the observations from two former dairy cow in vivo toxicokinetic experiments. We used Lorenzi et al.'s (2020) dairy cow experimentation for the fitting of *Cont k_{met}* of all PCB congeners, as well as 2,3,7,8-TCDD, 2,3,7,8-TCDF, and 1,2,3,7,8,9-HxCDF, whereas Huwe and Smith's (2005) dataset was used for the 14 other PCDD/F congeners. Experimental designs (i.e. exposure and depuration time frame, cow milk yield, intake level, and composition of the diet) were reproduced in the model setting, based on the details provided in the source articles (Huwe and Smith, 2005; Lorenzi et al., 2020) and summarised in Table 2. Once *Cont k_{met}* was fitted to one of the datasets, the predictive
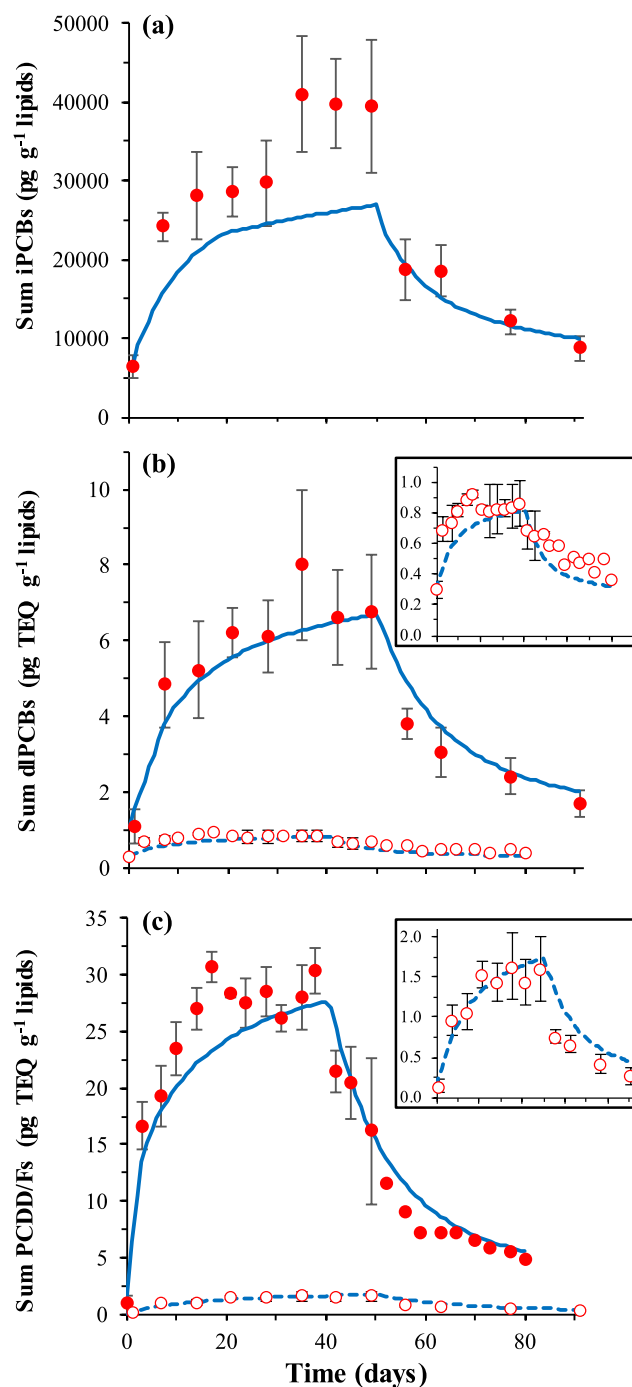
Fig. 2. Accumulation and depuration kinetics of milk concentrations in sums of indicator polychlorinated biphenyls (iPCBs, panel a), dioxin-like PCBs (dlPCBs, panel b), and polychlorinated dibenzo-p-dioxins and dibenzofurans (PCDD/Fs, panel c). Values are experimentally observed (red circle symbol) or simulated by the lactating cow RuMoPOP model (blue curve) at the fitting (filled symbol and full curve) or evaluation (open symbol and dotted curve, and framed zoom with adjusted scale on the right side) steps against the Lorenzi et al. (2020, 49 days exposure, 42 days depuration) or Huwe and Smith (2005, 40 days exposure, 40 days depuration) toxicokinetic experiments.

capabilities of the model were evaluated by comparing its simulations against the dataset of the second study. Accordingly, Lorenzi et al.'s (2020) study was used as an external evaluation dataset for the 14 PCDD/F congeners fitted to Huwe and Smith's (2005) data, and conversely, the latter study was used to evaluate the model predictive capabilities for PCBs 126 and 169, initially fitted to the Lorenzi et al.'s

(2020) data.

Model goodness of fit and accuracy were assessed using various evaluation parameters (Tedeschi, 2006) computed with the R software (version 3.6.3, R Core Team, 2020). Accuracy measures how closely model-predicted values are to the observed values (Tedeschi, 2006). Linear regression between predicted and observed values determined the coefficient of determination (R^2) that is indicative of model goodness of fit; whereas root mean square error of prediction (RMSE), and RMSE relative to the observed mean (RRMSE) are metrics of model accuracy. The mean square error of prediction (MSEP) was further decomposed into error proportions due to central tendency (ECT, accuracy indicator), regression (ER), and disturbance (ED, random error, with a low value indicative of lack-of-fit; Tedeschi, 2006). The mean bias (MB) was computed as the mean difference between observed and model-predicted values (Tedeschi, 2006) and the mean absolute percentage error (MAPE) as the mean of the absolute MB relative to the observed values (Cheng et al., 2016), and both are indicative of model accuracy. The overall goodness of fit of the model was judged acceptable when the R^2 was equal to or higher than 0.75 (Li et al., 2018), and when ED was equal to or higher than 60 %. Accuracy was judged satisfactory when predictions fell within a factor of two of the observations (WHO, 2010), when the absolute MB relative to the observed mean and the MAPE was equal to or lower than 25 % and 50 %, respectively (Li et al., 2018), and when RMSE was lower than the standard deviation (SD) of the observations, and RRMSE was equal to or lower than 50 % (Cheng et al., 2016).

2.3. Model application

Application of the model consisted of studying the interplay between the contaminant properties, cow productivity, and type of diet on milk and adipose tissue toxicokinetics. Simulation settings included the comparison of the toxicokinetics of four theoretical contaminants diverging in lipophilicity (mid: Mid_Lip or high: High_Lip; *Cont K_{ow}* of 10^6 and $10^{8.5}$, respectively) and metabolic clearance (none: Un_Met or moderate: Mod_Met; *Cont k_{met}* of 0 or 5 day^{-1}) chosen within the ranges of PCBs and PCDD/Fs (Table 2). The setting considered two types of lactating cow (low- or high-yielding, *POT* of 10 or 50 kg day^{-1}) fed with one of three different diets (with or without supplementation at 5 % dry matter intake with absorbable lipids, i.e. vegetable oil, or non-absorbable lipids, e.g. mineral oil). Details of the simulation setting are provided in Supplementary Table S1. All the 24 combinations (four contaminants × two cow productivities × three diets) were simulated according to a constant exposure scenario with a diet contaminant concentration set at 0.40 ng kg^{-1} dry matter (UE action threshold for the sum toxic-equivalent of dlPCBs in feed, Regulation EU n°277/2012) over three consecutive lactations. To compare the accumulation rates of lipophilic contaminant into milk according to the 24 combinations, the transfer rate from oral intake to milk was computed at 150 days in milk in the third lactation, according to Equation (6):

compare depuration rates of lipophilic contaminant into milk according to the 24 combinations, two-phased exponential decay models were adjusted to the simulated milk contaminant concentrations using the NLIN procedure of the SAS software (version 9.4, SAS Institute Inc., NC) and the following model (Driesen et al., 2022a):

$$C_t \ (\text{pg g}^{-1}\text{lipids}) \ = \ C_{0\alpha} \ (\text{pg g}^{-1} \text{ lipids}) \ \times \ \exp^{-\alpha \ (\text{day}^{-1}) \ \times \ t \ (\text{day})}$$
$$+ \ C_{0\beta} \ (\text{pg g}^{-1} \text{ lipids}) \ \times \ \exp^{-\beta \ (\text{day}^{-1}) \ \times \ t \ (\text{day})}$$

(7)

where C_t is the milk contaminant concentration at a given time t, $C_{0\alpha}$ and $C_{0\beta}$ the initial contaminant concentration of the fast and long elimination phases, respectively, and α and β the corresponding decay rate constants. The half-life for each component was further defined as:

$$\text{Half} - \text{life (day)} \ = \ \ln(2) \ / \ \alpha \text{ or } \beta \ (\text{day}^{-1})$$

(8)

3. Results

3.1. Model fitting and predictive capabilities for PCBs and PCDD/Fs

The model fitting against biological observations of milk accumulation and depuration kinetics for the sums of iPCBs, dlPCBs, and PCDD/Fs are illustrated in Fig. 2. The fitting for six individual congeners representative of the ranges in *Cont K_{ow}* and *Cont k_{met}* (i.e. PCBs 81, 126, and 180, 2,3,4,7,8-PeCDF, 1,2,3,4,6,7,8-HpCDF, and OCDF) are additionally reported in Fig. 3. Supplementary Table S2 reports the detailed statistics characterising model adequacy for all the single congeners and sums. At both the fitting and evaluation steps, a satisfactory goodness of fit of model predictions compared to observations was recorded for all the sums and for some individual congeners based on visual appreciation. Typical bi-exponential accumulation and depuration kinetics were observed in the experimental observations and were well reproduced by the model simulations (Figs. 2 and 3). The overall goodness of fit was confirmed quantitatively with ED (i.e. RMSE decomposition not attributed to ECT and ER) equal to or higher than 60 % for two third and half of the individual congeners at the fitting and evaluation steps, respectively (Supplementary Table S2). The model accuracy was judged satisfactory based on absolute MB relative to the observed mean, most of the time equal to or lower than 25 % (51 out of 56 individual congeners or sums) and always lower than 40 %. Moreover, for individual time-point comparison, 90 % of the model predictions fell within a factor of two of the experimental observations (i.e. 0.5 × observation ≤ prediction ≤ 2.0 × observation for 724 out of 803 comparisons). Remarkable exceptions were PCBs 101 and 77 at the fitting step and 1,2,3,4,7,8,9-HpCDF at the evaluation step, with 6–7 out of 11 comparisons outside a factor of two of the observations. Accordingly, MAPE from 98–343 % were recorded for these specific congeners compared to the others and the sums (i.e. 51 out of 56 MAPE equal of lower than 50 %).

In the fitting step, the model goodness of fit was mostly judged satisfactory, with both $R^2 \geq 0.75$ and RRMSE ≤ 40 % for 28 out of 38

$$\text{Transfer rate } (\%) \ = \ \big[\text{Milk contaminant concentration } (\text{pg g}^{-1} \text{ lipids})$$
$$\times \ \text{Milk lipid yield } (\text{g day}^{-1}) \big] \ / \ \big[\text{Diet contaminant concentration } (\text{ng kg}^{-1} \text{ dry matter}) \ \times \ \text{Dry matter intake} (\text{kg d}^{-1}) \big]$$
$$\times \ 100$$

(6)

Additionally, a depuration scenario (diet contaminant concentration of 0.05 ng kg^{-1} dry matter) was investigated according to the 24 combinations, starting at 100 days in milk in the third lactation after constant exposure (0.40 ng kg^{-1} dry matter) with the non-supplemented diet. To

congeners and sums. Only PCBs 28, 52, 101, and 77, as well as 2,3,7,8-TCDF, together showed $R^2 \leq 0.50$ and RRMSE ≥ 60 %, despite the fact that only the latter had an RMSE higher (1.1-fold) than the SD of the observations. This last feature only applied to two other congeners, that is, PCBs 156 and 167, with respective RMSE of 1.4- and 1.1-fold of the
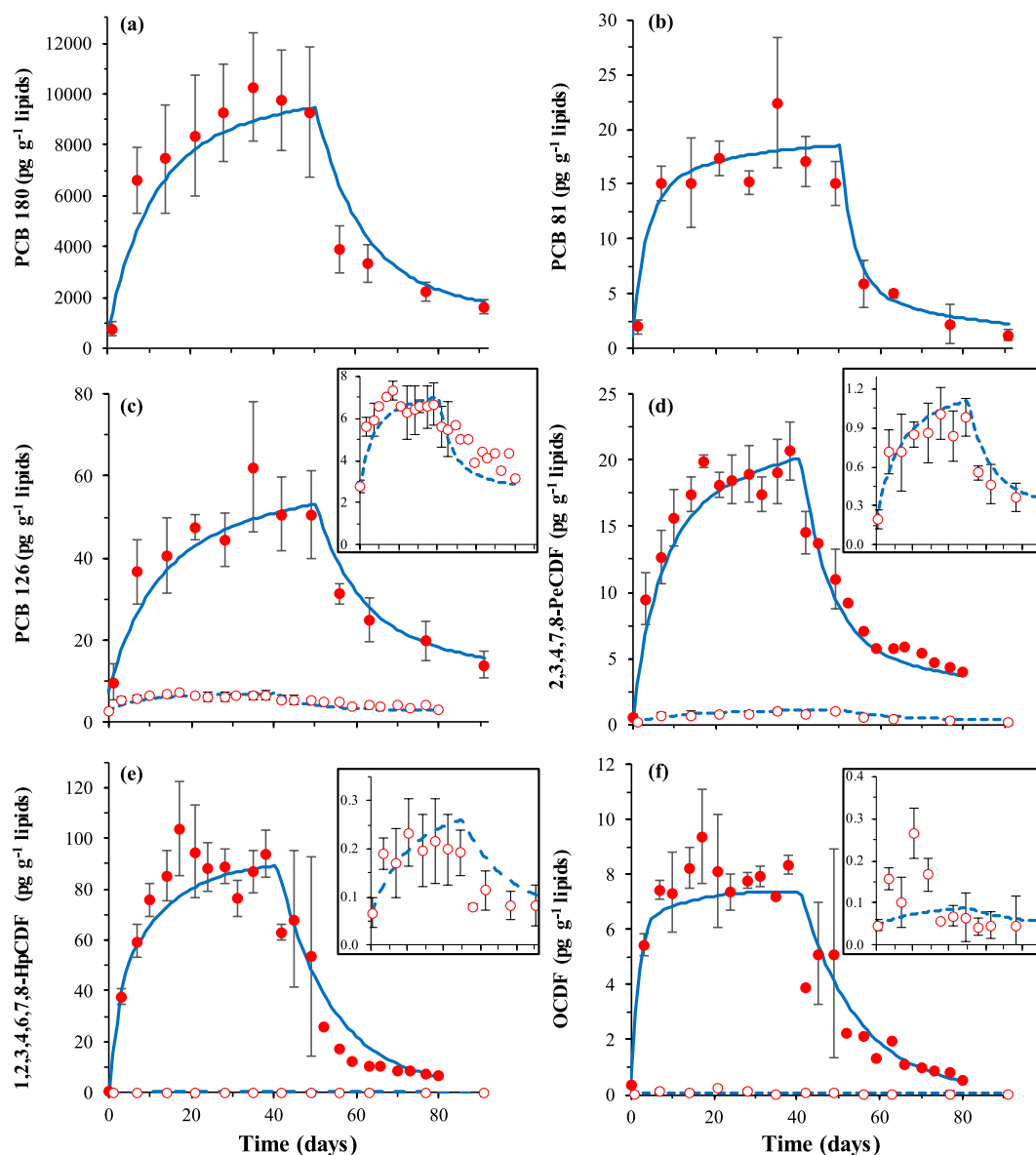
Fig. 3. Accumulation and depuration kinetics of milk concentrations in individual congeners of polychlorinated biphenyls (PCBs 180, 81, and 126, panels a, b, and c, respectively) and dibenzofurans (2,3,4,7,8-PeCDF, 1,2,3,4,6,7,8-HpCDF and OCDF, panels d, e, and f, respectively). Values are experimentally observed (red circle symbol) or simulated by the lactating cow RuMoPOP model (blue curve) at the fitting (filled symbol and full curve) or evaluation (open symbol and dotted curve, and framed zoom with adjusted scale on the right side) steps against the Lorenzi et al. (2020), 49 days exposure, 42 days depuration) or Huwe and Smith (2005, 40 days exposure, 40 days depuration) toxicokinetic experiments.

observation SD. At the evaluation step, goodness of fit was also satisfactory when judged on an RMSE basis, with a range similar to that at the fitting step. Only 1,2,3,4,7,8,9-HpCDF and OCDF had RRMSE higher than 50 %, and PCB 169 and 1,2,3,4,6,7,8-HpCDD showed RMSE values of 1.1- and 1.8-fold of the observation SD, respectively (out of 18 individual congeners or sums). Conversely, lower R^2 values were recorded with only four individual congeners and the two sums with values higher than 0.75 (Supplementary Table S2).

3.2. Model application

3.2.1. Effects of cow productivity and dietary lipids on body, milk, and faecal lipid dynamics

The main physiological traits of low- and high-yielding lactating cows producing 10 or 50 kg day^{-1} milk, respectively, at the lactation peak are illustrated in Supplementary Fig. S1. According to the

simulations of the physiological sub-model, the low-yielding cow had 2- and 5-fold lower feed intake and milk lipid yield, respectively, compared to the high-yielding cow. Decreases in BW and empty body lipid mass in early lactation and subsequent increases after 100 days in milk were more pronounced in high- than low-yielding cows, leading, on average, to 1.1- and 1.5-fold higher BW and body lipid mass in low-yielding cows during lactation. The decreases of milk lipid yield and raw milk yield from 50 days in milk onwards also showed a faster decay rate for high-yielding cows than for low-yielding cows, on an absolute amount basis, whereas proportional decreases from 50 to 300 days in milk were of similar magnitude whatever the cow productivity (2.3 and 2.2-fold decrease for milk lipid yield, and 3.1 ad 2.4-fold decrease for raw milk yield, for high- and low-yielding cows, respectively). By design of the physiological sub-model, absorbable or non-absorbable lipid supplementations had no effect on feed intake, milk yield, or body lipid dynamics (data not shown); they only modulated the lipid dynamics in the
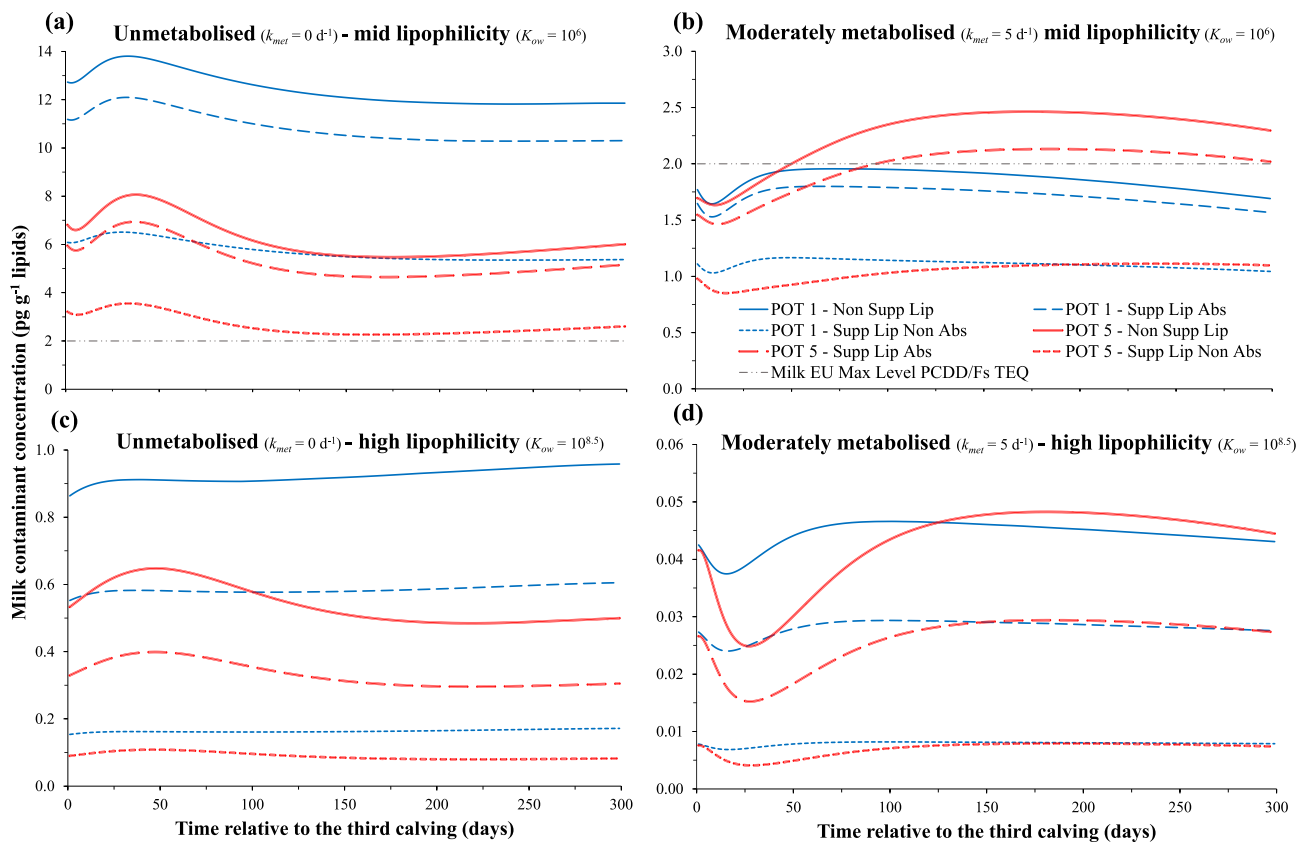
Fig. 4. Effects of lactating cow physiology and diet lipid content and digestibility on the milk accumulation kinetics. Lactating cows produce 10 (POT 1) or 50 kg milk d^{-1} (POT 5) at the lactation peak. Diets are non-supplemented (Non Supp Lip) or supplemented with 5 % lipids in dry matter intake, either absorbable (Supp Lip Abs, 89 % digestibility) or non-absorbable (Supp Lip Non Abs, 0 % digestibility). Theoretical contaminants are of mid lipophilicity (coefficient of partition between octanol and water, *Cont* K_{ow} 10^6) and unmetabolised (metabolic first-order clearance rate in the liver, *Cont* k_{met} 0 d^{-1}, panel a), of mid lipophilicity and moderately metabolised (*Cont* k_{met} 5 d^{-1}, panel b), of high lipophilicity (*Cont* K_{ow} $10^{8.5}$) and unmetabolised (panel c), or of high lipophilicity and moderately metabolised (panel d). Contamination scenarios were simulated over three consecutive lactation-gestation cycles with a fixed diet contaminant concentration of 0.40 ng kg^{-1} dry matter (European action threshold for the toxic-equivalent sum of dioxin-like polychlorinated biphenyls, Regulation EU n°277/2012). Kinetics during the third lactation are illustrated.

digestive tract, with further consequences only on the absorption and faecal excretion of lipophilic contaminants (see Sections 3.2.3 and 3.2.4). Compared to the non-supplemented diet and regardless of cow productivity, supplementation with absorbable or non-absorbable lipids at 5 % of the total dry matter intake increased by 1.7- and 6.6-fold, respectively, the amounts of lipids in the digestive tract and excreted through faeces.

3.2.2. Temporal trends in the accumulation kinetics of lipophilic contaminants across successive lactations

The accumulation kinetics in milk of the four theoretical contaminants with diverging ADME properties (lipophilicity and metabolic clearance rate) in a high-yielding cow are illustrated along three successive lactations in Supplementary Fig. S2. Starting from a theoretical initial contaminant body burden of 0 pg at the time of the first calving, the milk concentrations increased sharply over the first lactation for a Mid_Lip and Un_Met contaminant, up to 5.9 pg g^{-1} lipids at the end of lactation (300 days in milk). A similar pattern was observed for Mid_Lip and Mod_Met (*Cont* k_{met} of 5 day^{-1}) or High_Lip and Un_Met contaminants, but they only reached moderate concentrations at the end of lactation (2.3 and 0.4 pg g^{-1} lipids, respectively). Conversely, High_Lip and Mod_Met contaminants remained at very low milk concentrations (0.04 pg g^{-1} lipids at 300 days in milk). Regardless of the contaminant properties, a close pattern in the milk kinetics was observed within each of the second and third lactation cycles. Milk contaminant concentration first dropped over the first 5–20 days post

calving and then increased to peak around 40 and 115 days in milk for Un_Met and Mod_Met contaminants, respectively. Furthermore, a more or less pronounced decrease in milk concentration for Un_Met or increase for Mod_Met, depending on the contaminant lipophilicity, occurred up to 200 days in milk, with concentrations subsequently remaining almost stable until the end of lactation. Unless variations occurred during lactation, the milk contaminant concentration remained within narrow ranges and never deviated from the lowest to the highest concentrations recorded over the third lactation, with more than 1.1-fold for High_Lip and up to 1.5-fold for Mid_Lip contaminants (Supplementary Fig. S2).

3.2.3. Effects of contaminant properties, cow productivity, and dietary lipids on lipophilic contaminant accumulation kinetics

The milk accumulation kinetics of the four theoretical contaminants during the third lactation, considering cow productivity and dietary lipid supplementation, are illustrated in Fig. 4, and the corresponding kinetics in adipose tissue are reported in Supplementary Fig. S3. Oral intake to milk transfer rates at mid-lactation (150 days in milk) are reported in Table 3. The amplitude of increase and decrease in both milk and adipose tissue concentrations during the third lactation described above varied across the two cow productivities, being the highest in high-yielding cows and lowest in low-yielding cows. Cow productivity also widely impacted the milk and adipose tissue concentrations, averaged for the whole lactation of Un_Met contaminants but only marginally for Mod_Met contaminants. For the non-supplemented diet and

Table 3

Model simulated transfer rates and short (α) and long (β) depuration half-lives in milk for theoretical contaminants of mid or high lipophilicity, and unmetabolised or moderately metabolised, depending on cow milk productivity and diet lipid content and digestibility (4 contaminants × 2 cow milk production levels × 3 diet lipid levels and digestibility: $n = 24$ combinations).[1]

Contaminant[2]		POT 1			POT 5		
log K_{ow}	k_{met} (d⁻¹)	Non Supp Lip	Supp Lip Abs	Supp Lip Non Abs	Non Supp Lip	Supp Lip Abs	Supp Lip Non Abs
Transfer rate (%)[3]							
6.0	0	86	74	39	89	76	37
6.0	5	14	12	8	40	34	17
8.5	0	6.5	4.1	1.1	8.2	5.0	1.4
8.5	5	0.3	0.2	0.1	0.8	0.5	0.1
α depuration half-life (d)[4]							
6.0	0	30	29	23	20	19	17
6.0	5	5.3	5.2	4.9	3.4	3.3	2.9
8.5	0	*58*	*59*	*54*	48	47	46
8.5	5	13.8	13.6	13.4	8.9	8.8	8.7
β depuration half-life (d)[4]							
6.0	0	398	355	233	231	197	105
6.0	5	72	70	60	35	33	24
8.5	0	573	517	436	613	456	317
8.5	5	*2082*	*2350*	*1120*	*807*	*613*	*248*

In italics, the half-life for which the intercept value of the exponential compartment was less than 20% of the corresponding intercept value of the other exponential compartment.

[1]POT defines the cow productivity with milk yield at the lactation peak of 10 or 50 kg d⁻¹ for POT 1 and POT 5, respectively. Diet is non-supplemented with lipids (Non Supp Lip), supplemented with 5 % of absorbable lipids (i.e. vegetable oil of 89 % digestibility, Supp Lip Abs), or supplemented with 5 % of non-absorbable lipids (i.e. mineral oil of 0 % digestibility, Supp Lip Non Abs).

[2]log K_{ow}: Decimal logarithm of the partition coefficient between octanol and water. 10^6 corresponds to mildly and $10^{8.5}$ highly lipophilic contaminants. k_{met}: First order metabolic clearance rate in the liver. 0 d⁻¹ corresponds to unmetabolised and 5 d⁻¹ to moderately metabolised contaminants.

[3]Transfer rate is defined as the daily milk excretion to oral intake ratio of contaminant amounts. It is computed at 150 days in milk in the third lactation [intake of 11.2 and 23.9 kg dry matter (DM) d⁻¹, and milk lipid yield of 0.27 and 1.34 kg d⁻¹, for POT 1 and POT 5, respectively], after constant exposure (diet at 0.40 ng kg⁻¹ DM) since the first calving.

[4]A bi-exponential decay model—$C_t = a \times \exp(-\alpha \times t) + b \times \exp(-\beta \times t)$—was adjusted to the milk contaminant concentration during the depuration period (diet at 0.05 ng kg⁻¹ dry matter) from 100 to 300 days in milk in the third lactation, after constant exposure (diet at 0.40 ng kg⁻¹ dry matter, European action threshold for the toxic-equivalent sum of dioxin-like polychlorinated biphenyls, Regulation EU n°277/2012) from the first calving. α and β half-lives are for the fast and long exponential compartments and equal to ln(2)/α and ln(2)/β, respectively.

compared to high-yielding cows, milk concentrations of Un_Met contaminants were 2.0-fold higher for Mid_Lip, and 1.7-fold higher for High_Lip contaminants in low-yielding cows. In adipose tissue, the Un_Met and Mid_Lip contaminant concentrations were also 2.0-fold higher in low-yielding cows than in high-yielding cows but did not differ for High_Lip. Nonetheless, only slight effects of cow productivity were observed on the transfer rates to milk of Un_Met contaminants (86 to 89 % and 6.5 to 8.2 % for Mid_Lip and High_Lip, respectively). Conversely, milk concentrations of Mod_Met contaminants were lower and never deviated across cow productivities more than 1.2-fold, whereas their transfer rates increased almost 3-fold from low- to high-yielding cows. Concentrations of Mod_Met and Mid_Lip contaminant concentrations in adipose tissue were also similar across cow productivities (i.e. within a 1.4-fold range).

Consistent decreasing effects of diet lipid supplementation on milk and adipose tissue contaminant concentrations and milk transfer rates were observed, regardless of the contaminant properties and cow productivity. Regardless of the contaminant metabolic clearance, decreases in concentrations and transfer rates were the highest when the diet was supplemented with non-absorbable lipids, from around 2.0-fold for Mid_Lip contaminants, up to 5.8-fold for High_Lip contaminants, compared to the non-supplemented diet. By contrast, decreases were only moderate (1.2- and 1.6-fold for Mid_Lip and High_Lip, respectively) in the diet supplemented with absorbable lipids. Altogether, the highest concentrations of 13.8 and 14.4 pg g⁻¹ lipids in milk and adipose tissue, respectively, were recorded for Un_Met and Mid_Lip contaminants in early-lactation of low-yielding cows fed a non-supplemented diet (Fig. 4 and Supplementary Fig. S3).

3.2.4. Effects of contaminant properties, cow productivity, and dietary lipids on lipophilic contaminant depuration kinetics

The depuration kinetics of the four contaminants in milk from 150 days in milk in the third lactation, considering cow productivity and dietary lipid supplementation, are illustrated in Fig. 5, and the corresponding kinetics in adipose tissue are reported in Supplementary Fig. S4. The short- and long-term half-lives in milk are reported in Table 3, and the detailed intercept and slope parameters of the bi-exponential milk depuration kinetics are reported in Supplementary Table S3. Contaminant metabolic clearance was highlighted as the main determinant of the depuration rate, even if it is less pronounced in adipose tissue than in milk. Indeed, regardless of cow productivity, milk and adipose tissue depuration rates were remarkably shorter for Mod_Met contaminants, with 4.2- to 6.6-fold shorter α (fast distribution) and β (long elimination) half-lives compared to Un_Met contaminants for the non-supplemented diet. To a lesser extent, increases in contaminant lipophilicity led to a longer depuration rate, with milk half-lives that were 1.4- to 2.7-fold longer for High_Lip than for Mid_Lip contaminants. A similar range of modulation in the depuration rates was recorded due to cow productivity—that is, 1.2- to 2.6-fold shorter half-lives in high-yielding cows compared to low-yielding cows fed the non-supplemented diet—, regardless of the contaminant metabolic clearance and lipophilicity.

Diet supplementation with non-absorbable lipids hastened the depuration of Mid_Lip contaminants in milk and adipose tissue, especially the milk β half-life, which was shortened by 1.7- to 2.2-fold and 1.2- to 1.5-fold for Un_Met and Mod_Met contaminants, respectively, compared to the non-supplemented diet. By contrast, the effects of non-absorbable lipid supplementation on the milk α half-life and of absorbable lipid supplementation on milk and adipose tissue depuration kinetics were slight, with decreases in the range 1.0–1.3-fold for Mid_Lip contaminants. In the case of High_Lip contaminants, the effects of lipid supplementations on adipose tissue depuration kinetics as well as on milk α half-life were not perceivable, and only the milk β half-life of Un_Met contaminants was shortened by 1.3-fold in low-yielding cows and by
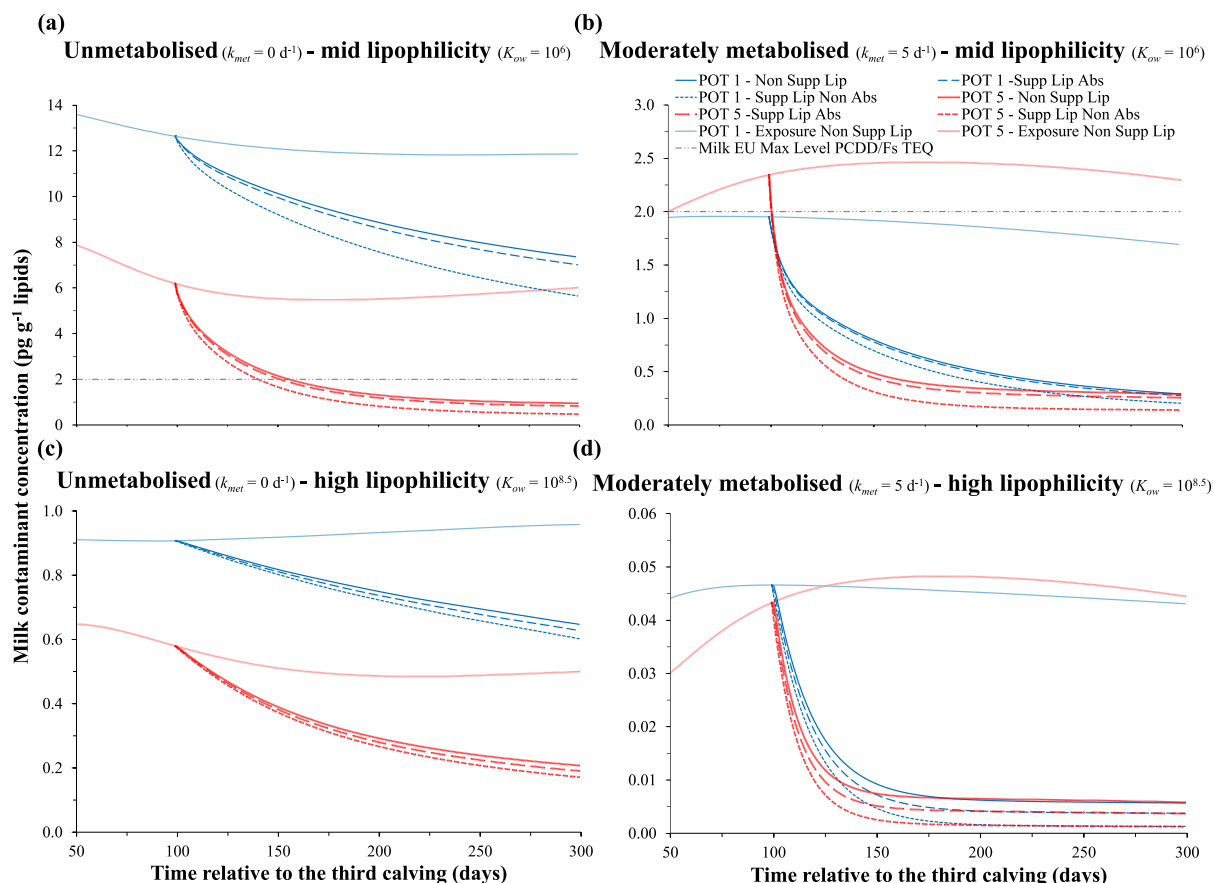
Fig. 5. Effects of lactating cow physiology and diet lipid content and digestibility on the milk depuration kinetics. Lactating cows produce 10 (POT 1) or 50 kg milk d^{-1} (POT 5) at the lactation peak. Diets are non-supplemented (Non Supp Lip) or supplemented with 5 % lipids in dry matter intake, either absorbable (Supp Lip Abs, 89 % digestibility) or non-absorbable (Supp Lip Non Abs, 0 % digestibility). Theoretical contaminants are of mid lipophilicity (coefficient of partition between octanol and water, *Cont K_{ow}* 10^6) and unmetabolised (metabolic first-order clearance rate in the liver, *Cont k_{met}* 0 d^{-1}, panel a), of mid lipophilicity and moderately metabolised (*Cont k_{met}* 5 d^{-1}, panel b), of high lipophilicity (*Cont K_{ow}* 10$^{8.5}$) and unmetabolised (panel c), or of high lipophilicity and moderately metabolised (panel d). Depuration scenarios were simulated from 100 days in milk in the third lactation with a fixed diet contaminant background concentration of 0.05 ng kg^{-1} dry matter after constant exposure (0.40 ng kg^{-1} dry matter, European action threshold for the toxic-equivalent sum of dioxin-like polychlorinated biphenyls, Regulation EU n°277/2012) with the Non Supp Lip diet from the first calving. For comparison purposes, the scenario of constant exposure with the Non Supp Lip diet until the end of the third lactation is additionally reported (light full lines noticed "Exposure Non Supp Lip").

1.9-fold in high-yielding cows due to non-absorbable lipid supplementation (1.1- and 1.3-fold for absorbable lipid supplementation, respectively). Altogether, the shortest milk half-lives of 2.9 days for α and 24 days for β were recorded for Mod_Met and Mid_Lip contaminants in high-yielding cows fed a diet supplemented with non-absorbable lipids.

4. Discussion

4.1. Novelty and limitations of the RuMoPOP model

A new dynamic and compartmental model, RuMoPOP, describes the toxicokinetic of lipophilic contaminant in lactating cows based on the combination of fugacity and physiologically based formalisms. The novelty of the proposed model is reflected by the coupling of a mechanistic ADME sub-model with a physiological sub-model that describes the cow's feed intake, lipid digestion, gestation, and lactation. This extends the model's use to several lipophilic contaminants in various production systems, from low-yielding suckler beef to high-yielding dairy cows, fed different diets varying in lipid content and digestibility. Previous attempts to provide generic PBTK model for lactating cow, encompassing at once the fine description of ADME and animal physiology, were achieved recently for oxytetracycline (Tardiveau et al., 2022) and per- and polyfluoroalkyl substances (Chou et al., 2023). The present RuMoPOP model provide an additional

attempt for genericity applied to lipophilic and apolar contaminants (e. g. PCBs and PCDD/Fs).

The need for only two input parameters to specify the characteristics of the targeted contaminant—that is, its lipophilicity (*Cont K_{ow}*) and metabolic clearance rate (*Cont k_{met}*)—is an important aspect of the model's ability to capture the fate of diverse lipophilic contaminants. The *Cont K_{ow}* is, in most cases, accessible from chemical properties databases (e.g. Mackay, 2001) and drives the contaminant absorption rate and its distribution delay to the deep adipose tissues, according to passive diffusion flows in series (McLachlan, 1994). Biological observations suggest that the *Cont K_{ow}* also governed the contaminant transfer at the blood to udder interface. In a first instance, and due to the scarcity of data reporting at once blood and milk concentrations of lipophilic contaminants in ruminant species, a correction factor *Cont $Corr P_{udder}$* was simply introduced in order to compensate for such diffusive resistance (Supplementary Information S2). Nonetheless, it would be more appropriate to represent the lipophilic contaminant flows at the blood to udder interface according to passive diffusion, in a way analogous to the digestive contents to blood and perfused to deep adipose tissues interfaces. Further studies and data characterizing the lipophilic contaminant partition and flows between blood, udder and milk would be needed to achieve this additional development of the RuMoPOP model. Such detailed representation of the contaminant transfer from blood to milk, and inside the mammary gland was formerly achieved in

cow PBTK models for antibiotics administrated intra-muscularly or intra-mammary (Tardiveau et al., 2022; Woodward and Whittem, 2019).

Contaminant distribution among the other tissues (partition co-efficients, $P_{tissue\ i}$) further depends on their respective lipid contents, assuming that apolar lipophilic contaminants diffuse almost exclusively into total lipids. Such an assumption excludes situations where lipophilic contaminants have functional groups (e.g. carbonyl such as chlordecone, Belfiore et al., 2007, or sulfonyl such as per- and poly-fluoroalkyl substances, Kowalczyk et al., 2013; Mikkonen et al., 2023), which also distribute into more polar lipids (e.g. phospholipids, free cholesterol) or bind to specific proteins. For such polar contaminants, the model would need to be adjusted by empirically fitting the partition coefficients ($P_{tissue\ i}$) as data on tissue distribution become available. Similarly, the metabolic clearance rate ($Cont\ k_{met}$) has to be adjusted for every contaminant, which was performed for PCBs and PCDD/Fs based on empirical fitting against in vivo experimental datasets (Huwe and Smith, 2005; Lorenzi et al., 2020).

Along the initial development of the RuMoPOP model, none variability was included on input parameters. This is mainly due to the scarcity of data available in the literature to fix some of the mechanistic parameters. This limitation did not allow providing uncertainties on model simulations (e.g. confidence intervals with probabilistic distributions and Monte-Carlo simulations, Chou et al., 2023; Tardiveau et al., 2022).

4.2. Model fitting and evaluation for PCBs and PCDD/Fs

An initial step of implementation (i.e. fitting and partial evaluation steps) of the RuMoPOP model was performed for the 18 PCB and 17 PCDD/F congeners regulated in feed (Regulation EU n°277/2012) and food of animal origin (Regulation EU n° 1259/2011). The model showed very satisfactory goodness of fit at model adjustment (i.e. optimisation against the dataset that serves for model fitting) and evaluation (i.e. predictive capabilities against an external dataset) and for most of the PCB and PCDD/F congeners. An exception was the R^2 values between model predictions and experimental observations (indicator of model goodness of fit), which were mostly judged unsatisfactory (≤ 0.75) at the evaluation step. This may be explained, at least partly, by the low values and reduced ranges of observed milk concentrations in PCBs 126 and 169 (Huwe and Smith, 2005) and PCDD/Fs (Lorenzi et al., 2020) that were used for the evaluation step.

Previously, only Bogdal et al. (2017) and Moenning et al. (2023a) adjusted the toxicokinetic models of lactating cows for the whole set of regulated PCBs and PCDD/Fs, whereas Tremolada et al. (2014) and Moenning et al. (2023c) did so for iPCBs (only PCBs 138, 153, and 180 in the later study). None of these previous studies examined model predictive capabilities against independent datasets (i.e. only results of optimisation were appreciated). Furthermore, only Tremolada et al. (2014) quantitatively assessed model accuracy; visual and qualitative assessments were performed in the other studies (Bogdal et al., 2017; Moenning et al., 2023a; Moenning et al., 2023c). Thus, similar (Moenning et al., 2023a; Moenning et al., 2023c; Tremolada et al., 2014) or lower (Bogdal et al., 2017) model predictive capabilities may be deciphered in previous studies compared to the present RuMoPOP model. Moenning et al. (2023a) judged their model for the prediction of the accumulation and depuration kinetics of PCBs and PCDD/Fs in milk as very satisfactory (score of 5 on a 1 to 5 scale) for 20 congeners, and moderately satisfactory (scores of 2, 3, or 4) for 12 out of 32 congeners. By applying McLachlan's (1994) cow fugacity model to the case study of dairy cows on high-mountain pasture, Tremolada et al. (2014) obtained a fair accuracy for PCBs 28, 52, 138, and 153 (absolute MB relative to the observed mean < 25 %, after fitting of the absorption and metabolic rates), which is similar to the accuracy obtained in the present study. Rosenbaum et al. (2009) and Takaki et al. (2015) also quantitatively evaluated the performance of the same fugacity model (McLachlan,

1994) for predicting the feed-to-milk transfer rate or biotransfer factor of several lipophilic contaminants (including PCDD/Fs and PCBs). The fugacity model adequacy was judged satisfactory and always better than empirical estimates from $Cont\ K_{ow}$-based linear (e.g. Travis and Arms, 1988) or non-linear (e.g. MacLachlan and Bhula, 2008) static models.

The metabolic clearance rate ($Cont\ k_{met}$) was the only model parameter adjusted by fitting against experimental data (Huwe and Smith, 2005; Lorenzi et al., 2020) at the optimisation step. The fitted $Cont\ k_{met}$ were the highest (> 100 d^{-1}) for PCBs 28, 52, and 101, high to moderate ($10\ d^{-1} < Cont\ k_{met} < 70\ d^{-1}$) for PCBs 77, 126, 2,3,7,8-TCDF, 1,2,3,7,8-PeCDF, and 1,2,3,7,8,9-HxCDF, and moderate to null ($0\ d^{-1} \leq Cont\ k_{met} < 5\ d^{-1}$) for the remaining 27 congeners. This ranking of metabolic susceptibility among PCB and PCDD/F congeners is in broad agreement with records of in vivo mass balances (extent of biotransformation) in lactating cows (Driesen et al., 2022b; McLachlan and Richter, 1998; McLachlan, 1993). Indeed, these studies suggested a ranking from well-metabolised (≥ 65 % of the contaminant oral intake was assumed to be eliminated by metabolism, e.g. PCBs 28, 52, 101, and 77), moderately metabolised (25–65 % metabolised, e.g. PCB 126 and tetra- and penta-chlorinated PCDD/Fs), and poorly-metabolised (≤ 25 % metabolised, e.g. PCBs 153, 180, and 189, hexa-, hepta- and octa-chlorinated PCDD/Fs) PCB and PCDD/F congeners (Driesen et al., 2022b; McLachlan and Richter, 1998; McLachlan, 1993). Only a few discrepancies between fitted $Cont\ k_{met}$ in the RuMoPOP model and metabolised fractions gathered from the Driesen et al. (Driesen et al., 2022b) experiment, were noticed for four penta-chlorinated PCBs, that is, 105, 114, 118, and 123. The ranking of hepatic metabolism susceptibility among PCBs and PCDD/Fs was also in broad agreement with the one in Bogdal et al.'s (2017) model, although lower values were found in the latter case (from 0.0010 d^{-1} for OCDD and OCDF, up to 0.0170 d^{-1} for PCBs 28 and 52). By contrast, the fitted $Cont\ k_{met}$ for PCB 52 (Tremolada et al., 2014) and 2,3,7,8-TCDD (Derks et al., 1994) of 181, and 14 d^{-1}, respectively, were of similar order of magnitude as in the present study (394, and 3 d^{-1}, respectively).

4.3. Interplay between contaminant properties, cow productivity, and dietary lipids on lipophilic contaminant toxicokinetics

Cyclic variation in contamination kinetic during lactation was more pronounced for Mid_Lip and Un_Met compared to High_Lip and Mod_Met contaminants, which may be explained by the low absorption and moderate metabolism rates of High_Lip and Mod_Met contaminants, respectively. Similarly, variation over a full lactation of the milk concentration was higher in the poorly metabolised PCB 153 than in the well-metabolised PCB 101 following long-term exposure of low-yielding cows (Driesen et al., 2022a). The cyclic pattern over lactation for Mid_Lip and Un_Met contaminants is explained by the temporal trends in body and milk lipid dynamics described by the physiological sub-model. The initial drop in the milk contaminant concentration in early lactation is mostly due to excretion through milk lipid secretion that is initiated at calving. Similarly, a drop in milk concentrations in PCBs and PCDD/Fs was observed across the first two weeks of lactation in cows exposed since day 109 prior to calving (Driesen et al., 2022a). Later model simulations of milk and adipose tissue contaminant concentrations showed increased and peaked around 100 days in milk, which is explained by the concomitant decrease in the body lipid mass (i.e. dilution space for lipophilic contaminants). Accordingly, the subsequent replenishment of body lipid reserves from mid-lactation drove the contaminant dilution and decreased its concentrations in milk and adipose tissue up to 200 days in milk. A similar increase and subsequent decrease in adipose tissue concentrations of PCBs and PCDD/Fs between 30 and 160 days in milk was observed in primiparous cows but was not perceivable in multiparous cows (Driesen et al., 2022a). Discrepancy between model simulations and biological observations may be explained by the only slight variation in the body lipid mass over lactation recorded in the experiment (Driesen et al., 2022a) compared to

the model-simulated cows. Indeed, the amplitude of variations in milk and adipose tissue concentrations was higher in high-yielding cows compared to low-yielding cows simulated by the model, with high and low intensity of body lipid mobilisation and replenishment, respectively, throughout lactation. Over the last third of lactation, milk and adipose tissue concentrations in Un_Met contaminants rose slightly again, according to model simulations. This may be explained by the concomitant linear decrease in milk lipid excretion, which is the almost exclusive route of elimination for body-stored Un_Met contaminants. This model insight is in accordance with the in vivo observation in low-yielding cows, where the milk concentrations in poorly metabolised PCBs and PCDD/Fs increased slightly from the mid to the end of lactation (Driesen et al., 2022a).

Concerning the effects of contaminant properties on accumulation and depuration, lipophilicity mostly affected contaminant absorption during exposure, as well as its redistribution from *Deep adipose tissues*, and faecal excretion following diffusion from *Blood* to *Digestive contents* during depuration. An increase in lipophilicity widely decreased the absorption rate along the exposure phase, with a curvilinear drop when *Cont* K_{ow} reached values over 10^7. Accordingly, an 85 % absorption rate for Mid_Lip contaminants (*Cont* K_{ow} of 10^6) but only 12 % for High_Lip contaminants (*Cont* K_{ow} of $10^{8.5}$) was reproduced by model simulations for diet non-supplemented with lipids. Similarly, only 3 % of the High_Lip and Un_Met contaminant body burden at the initiation of the depuration phase was excreted back from *Blood* to *Digestive contents*, compared to 52 % for Mid_Lip and Un_Met contaminant.

The fugacity-based representation of the absorption and non-biliary excretion at the *Digestive contents* to the *Blood* interface (McLachlan, 1994) implies a diffusive transfer of the contaminant into a water phase that figures the unstirred water layer surrounding the microvilli of the intestinal wall (Kelly et al., 2004). When contaminant solubility in water falls below a threshold (i.e. *Cont* $K_{ow} > 10^7$), the rates of absorption and non-biliary excretion decrease sharply. For the exposure phase, this fits very well with in vivo observations in lactating cows, in which, for example, Mid_Lip contaminants (*Cont* $K_{ow} \leq 10^6$) had an absorption rate around 80 %, compared to High_Lip contaminants (*Cont* $K_{ow} \geq 10^8$) with a 0–40 % absorption rate for PCBs and organochlorine pesticides (McLachlan, 1993), polybrominated diphenylethers (Kierkegaard et al., 2009), or PCBs and PCDD/Fs (Driesen et al., 2022b).

Following absorption, the contaminant metabolic clearance rate (*Cont* k_{met}) is the main parameter driving accumulation and depuration rates. Obviously, the increase in *Cont* k_{met} led to a wide decrease in accumulation and a sharp increase in the depuration rates of milk and body tissues. The increase from 0 to 5 day^{-1} of the *Cont* k_{met} of Mid_Lip contaminants decreased the milk transfer rate by 3-fold during the exposure phase, whereas it shortened the short-term α and long-term β milk half-lives by 5- and 4-fold during the depuration phase. These model insights are in accordance with in vivo observations by Lorenzi et al. (2020), Driesen et al. (2022a), and Krause et al. (2023a). For the exposure phase, PCBs 105 and 81 (Mid_Lip with *Cont* K_{ow} of $10^{6.6}$ and $10^{6.4}$, respectively), which have *Cont* k_{met} similar to that of Un_Met (0 day^{-1} for PCB 105) or Mod_Met (3 day^{-1} for PCB 81), had 2- to 3-fold differences in their milk transfer rates (33 % and 12 % in Lorenzi et al., 2020; 27 % and 15 % in Krause et al., 2023a, for PCB 105 and 81, respectively). For the depuration phase, the Un_Met contaminant PCB 105 had 2- to 3-fold longer α and β milk half-lives than the Mod_Met (*Cont* k_{met} of 2.2 day^{-1} and *Cont* K_{ow} of $10^{6.7}$) PCB 118 (Driesen et al., 2022a).

Besides the effects of the contaminant properties, the RuMoPOP model quantified the effect on the toxicokinetics of the cow feeding and physiology. The model application yielded insights into the effectiveness of diet supplementation with non-absorbable lipids to shorten the accumulation rate and hasten the depuration kinetics. Over both the exposure and depuration phases, contaminant absorption and faecal excretion were modulated by dietary lipid supplementation, whereas the milk productivity mostly affected body distribution and milk

excretion. During the exposure phase, supplementation of the diet with 5 % non-absorbable lipids dropped the absorption rate from 85 % to 46 % and from 12 % to 2 % for Mid_Lip and High_Lip contaminants, respectively. During depuration, such a feeding strategy led to an increase of 2.9- to 4.0-fold in the faecal excretion of Mid_Lip contaminants. This is explained by the concomitant increases in the lipid content of the *Digestive contents* and *Faecal excretion* of the lipid. The former increased the affinity of *Digestive contents*, displacing the *Digestive contents* to *Blood* concentration gradient, and the latter increased the *Faecal excretion* pathway for the lipophilic contaminant. By contrast, according to the model simulations, the effect of non-absorbable lipid supplementation on the increase in faecal excretion was only marginal for High_Lip contaminants (1.1- to 1.2-fold). This is explained by the high resistance of High_Lip contaminants to the diffusive transfer across the water layer of the intestinal wall.

Additionally, the effectiveness of lipid supplementation in hastening depuration was also shorter for Mod_Met than for Un_Met contaminants. This is explained by metabolic clearance, which is the primary route of elimination of Mod_Met contaminants, compared to the lower contribution of faecal excretion. Conversely, Un_Met contaminants are not metabolized, and faecal and milk excretion are therefore the only routes for their elimination. Similar insights regarding the effect of dietary non-absorbable lipids were previously gathered from in vivo investigations (Lerch et al., 2020; Rey-Cadilhac et al., 2020; Rozman et al., 1982; Rozman et al., 1984; Volpenhein et al., 1980). During the exposure phase, the partial substitution of soybean oil by sucrose polyester (i.e. olestra, a non-absorbable fat substance) in the diet of rats (in the total emulsion diet: 10 % sucrose polyester and 10 % soybean oil vs. 20 % soybean oil for the control group) decreased the lymphatic absorption of dichloro-diphenyl-trichloroethane (*Cont* K_{ow} of $10^{6.9}$) from 67 % to 21 % of the ingested dose (Volpenhein et al., 1980). Other studies have investigated the effect of non-absorbable lipid supplementation on the depuration kinetics of lipophilic contaminants in growing lambs (Rozman et al., 1982), lactating goats (Rozman et al., 1984), and non-lactating ewes (Lerch et al., 2020; Rey-Cadilhac et al., 2020). During the depuration phase, diet supplementation with 5–10 % (dry matter basis) mineral oil increased the faecal excretion of hexachlorobenzene (Rozman et al., 1982), mirex (Rozman et al., 1984), and PCBs 126, 153, and TCDD (Lerch et al., 2020; Rey-Cadilhac et al., 2020) by 2- to 3-fold. Furthermore, model insight regarding the divergent effect of non-absorbable lipid supplementation on the faecal excretion of body-stored Mid_Lip and High_Lip contaminants is also in accordance with a former experiment on PCBs, PCDD/Fs and hexachlorobenzene in humans (Moser and McLachlan, 1999). Human diet supplementation with 25 g day^{-1} of sucrose polyester increased the faecal excretion of body-stored Mid_Lip contaminants by 6- to 10-fold (*Cont* $K_{ow} \leq 10^6$), whereas that of High_Lip contaminants was increased but only by 1- to 2-fold (*Cont* $K_{ow} \geq 10^{8.5}$) (Moser and McLachlan, 1999).

According to the RuMoPOP model, cow milk productivity specifically affected the distribution and milk excretion of lipophilic contaminants. During the exposure phase, higher milk concentrations in Un_Met contaminants were observed in low-yielding cows than in high-yielding cows. Additionally, during depuration, low-yielding cows had longer milk half-lives than high-yielding cows. This is mostly explained by the enhanced Un_Met contaminant elimination through milk excretion in high-yielding cows than in low-yielding cows, allowed by the 5-fold higher milk lipid yield in the former. Accordingly, compared to low-yielding cows, the body burden in Un_Met contaminants of high-yielding cows was 2-fold lower after constant exposure over three successive lactations, whereas its decrease was around 2-fold higher across 200 days of depuration. Altogether, these model insights suggest that low-yielding cows, such as suckler beef cows, would be more sensitive to the risk of milk and body tissue contamination at high levels compared to high-yielding cows, such as dairy cows fed an intensive diet. By contrast, milk concentrations in Mod_Met contaminants were similar across cow milk productivity in both the exposure and depuration

phases (within a 1.2-fold range, on average, during the third lactation). Indeed, metabolic clearance is the main route of elimination of Mod_Met contaminants and occurred at a similar rate in low- and high-yielding cows with a similar body burden, regardless of the milk productivity and phase (within a 1.1-fold range). Furthermore, the RuMoPOP model reproduced the effect of cow physiology observed in the in vivo experiment of Driesen et al. (2022a, 2022b)). During exposure, 1.2-fold higher milk concentrations, on average, during lactation and 1.3-fold higher body burden at the end of lactation were recorded for the poorly metabolised PCB 153 in low-yielding primiparous cows (milk lipid yield of 0.44 kg day^{-1}) compared to mid-yielding multiparous cows (milk lipid yield of 0.59 kg day^{-1}). By contrast, no difference was observed in milk concentration or body burden for the highly metabolised PCB 101 (Driesen et al., 2022a, 2022b). Moreover, over 124 days of depuration, the long-term β half-life of PCB 153 in milk was 1.8-fold longer in low-yielding cows than in mid-yielding cows, whereas no depuration bi-exponential kinetics could be fitted for PCB 101, whose elimination curve was too flat due to high metabolic clearance (Driesen et al., 2022a). Additionally, according to the model simulations, a lower transfer rates to milk occurs in low- than high-yielding cows for most contaminants. This is also in accordance with biological observations for most of the PCB and PCDD/F congeners (Driesen et al., 2022a). Only exception was Un_Met and Mid_Lip contaminant with equivalent transfer rate to milk. This might be explained by their very high transfer rate to milk (86 % and 89 % in low- and high-yielding cows), meaning that at 150 days in milk in the third lactation, under a quasi-steady state situation, the amount of absorbed Un_Met and Mid_Lip contaminant distributed to the body burden is negligeable. Accordingly, the quasi totality of the daily absorbed Un_Met and Mid_Lip contaminant is eliminated through milk excretion, whatever the cow productivity.

5. Conclusion

Novel aspects of the present investigation include a fine-tuned description of the lipophilic contaminant ADME in the mechanistic RuMoPOP model based on fugacity and PBTK formalisms. The model application proved useful for testing several research hypotheses aimed at determining the main drivers of lipophilic contaminant accumulation and depuration kinetics in lactating cows. The model simulations recorded a higher accumulation rate for non-metabolised contaminants of mid lipophilicity in low-yielding cow fed diet non-supplemented with lipids, whereas faster depuration rates were recorded for moderately metabolised contaminants of mid lipophilicity in high-yielding cow fed diet supplemented with non-absorbable lipids. In practice, describing exposure and depuration scenarios on a case-by-case basis requires dynamic simulations, as the results of each combination of contaminant properties with cow physiology and feeding lead to specific outcomes. The exploration of such complex contaminant–animal interplay is allowed by the use of the mechanistic RuMoPOP model. To go deeper in such understanding, perspectives include a sensitivity analysis of the RuMoPOP model that would allow to decipher quantitatively the key toxicokinetic drivers depending on the contaminant-animal interplay.

During the initial development of the RuMoPOP model, empirical fitting of the hepatic clearance rate (*Cont k$_{met}$*) was performed against two in vivo experimental datasets for PCB and PCDD/F congeners, and the predictive abilities of the model were judged satisfactory. Future developments could adjust the model for additional legacies and emerging lipophilic contaminants. The unavailability of in vivo toxicokinetic data for specific contaminants in lactating cows for empirical fitting poses a challenge to assessing the reliability of deriving *Cont k$_{met}$* values based on new approach methods (NAMs, Klevenhusen et al., 2021; Reale et al., 2024). Such attempts may not only spare expensive resources and time but also reduce the dependency on animal experimentation, in line with the principles of the 3Rs (replacement, reduction, and refinement; Klevenhusen et al., 2021). As an additional perspective, the ultimate delivery of the RuMoPOP model as a user-friendly web-module for routine uses by risk assessors and managers is foreseen (e.g. ConTrans, https://contrans.bfr.bund.de/, BfR, Germany; Feed-food transfer, https://www.feedfoodtransfer.nl/en, RIVM, WUR, The Netherlands).

CRediT authorship contribution statement

Sylvain Lerch: Writing – review & editing, Writing – original draft, Visualization, Validation, Supervision, Project administration, Methodology, Investigation, Funding acquisition, Formal analysis, Conceptualization. **Olivier Martin:** Writing – review & editing, Resources, Methodology, Investigation, Conceptualization. **Agnés Fournier:** Writing – review & editing, Conceptualization. **Isabelle Ortigues-Marty:** Writing – review & editing, Resources. **Jérôme Henri:** Writing – review & editing, Visualization, Validation, Supervision, Project administration, Methodology, Conceptualization.

Declaration of generative AI and AI-assisted technologies in the writing process

The authors did not use any AI-assisted technologies for the writing of the work.

Declaration of competing interest

The authors declare that they have no known competing financial interests or personal relationships that could have appeared to influence the work reported in this paper.

Appendix A. Supplementary data

Supplementary data to this article can be found online at https://doi.org/10.1016/j.envint.2025.109509.

Data availability

The code of the model is provided online at https://doi.org/10.5281/zenodo.14218322. Data from model simulations will be made available on request.

References

Amutova, F., Delannoy, M., Baubekova, A., Konuspayeva, G., Jurjanz, S., 2021. Transfer of persistent organic pollutants in food of animal origin – Meta-analysis of published data. Chemosphere 262, 128351. https://doi.org/10.1016/j.chemosphere.2020.128351.

Armitage, J.M., Hughes, L., Sangion, A., Arnot, J.A., 2021. Development and intercomparison of single and multicompartment physiologically-based toxicokinetic models: Implications for model selection and tiered modeling frameworks. Environ. Int. 154, 106557. https://doi.org/10.1016/j.envint.2021.106557.

BAG, 2013. PCB und Dioxine in Lebensmitteln, in: Gesundheit Bf (Ed.), pp. 1-5.

Belfiore, C.J., Yang, R.S.H., Chubb, L.S., Lohitnavy, M., Lohitnavy, O.S., Andersen, M.E., 2007. Hepatic sequestration of chlordecone and hexafluoroacetone evaluated by pharmacokinetic modeling. Toxicology 234, 59–72. https://doi.org/10.1016/j.tox.2007.02.002.

Bogdal, C., Züst, S., Schmid, P., Gyalpo, T., Zeberli, A., Hungerbühler, K., Zennegg, M., 2017. Dynamic transgenerational fate of polychlorinated biphenyls and dioxins/furans in lactating cows and their offspring. Environ. Sci. Tech. 51, 10536–10545. https://doi.org/10.1021/acs.est.7b02968.

Cahill, T.M., Cousins, I., Mackay, D., 2003. Development and application of a generalized physiologically based pharmacokinetic model for multiple environmental contaminants. Environ. Toxicol. Chem. 22, 26–34.

Cheng, Y.-H., Lin, Y.-J., You, S.-H., Yan, Y.-F., How, C.M., Tseng, Y.-T., Chen, W.-Y., Liao, C.-M., 2016. Assessing exposure risks for freshwater tilapia species posed by mercury and methylmercury. Ecotoxicology 25, 1181–1193. https://doi.org/10.1007/s10646-016-1672-4.

Chou, W.-C., Tell, L.A., Baynes, R.E., Davis, J.L., Cheng, Y.-H., Maunsell, F.P., Riviere, J.P., Lin, Z., 2023. Development and application of an interactive generic physiologically based pharmacokinetic (igPBPK) model for adult beef cattle and lactating dairy cows to estimate tissue distribution and edible tissue and milk withdrawal intervals for per- and polyfluoroalkyl substances (PFAS). Food Chem. Toxicol. 181, 114062. https://doi.org/10.1016/j.fct.2023.114062.

Derks, H.J.G.M., Berende, P.L.M., Olling, M., Everts, H., Liem, A.K.D., de Jong, A.P.J.M., 1994. Pharmacokinetic modeling of polychlorinated dibenzo-p-dioxins (PCDDs) and furans (PCDFs) in cows. Chemosphere 28, 711–715. https://doi.org/10.1016/0045-6535(94)90222-4.

Driesen, C., Lerch, S., Siegenthaler, R., Silacci, P., Hess, H.D., Nowack, B., Zennegg, M., 2022a., Accumulation and decontamination kinetics of PCBs and PCDD/Fs from grass silage and soil in a transgenerational cow-calf setting. Chemosphere. 296, 133951. Doi: 10.1016/j.chemosphere.2022.133951.

Driesen, C., Zennegg, M., Morel, I., Hess, H.D., Nowack, B., Lerch, S., 2021. Average transfer factors are not enough: The influence of growing cattle physiology on the transfer rate of polychlorinated biphenyls from feed to adipose. Chemosphere 270, 129698. https://doi.org/10.1016/j.chemosphere.2021.129698.

Driesen, C., Zennegg, M., Rothacher, M., Dubois, S., Wyss, U., Nowack, B., Lerch, S., 2022b. Transgenerational mass balance and tissue distribution of PCBs and PCDD/Fs from grass silage and soil into cow-calf continuum. Chemosphere 307, 135745. https://doi.org/10.1016/j.chemosphere.2022.135745.

Efsa, 2018. Risk for animal and human health related to the presence of dioxins and dioxin-like PCBs in feed and food. EFSA J. 16. https://doi.org/10.2903/j.efsa.2018.5333.

Ferrell, C.L., Garrett, W.N., Hinman, N., 1976. Growth, development and composition of the udder and gravid uterus of beef heifers during pregnancy. J. Anim. Sci. 42, 1477–1489. https://doi.org/10.2527/jas1976.4261477x.

Hoogenboom, R., Traag, W., Fernandes, A., Rose, M., 2015. European developments following incidents with dioxins and PCBs in the food and feed chain. Food Control 50, 670–683. https://doi.org/10.1016/j.foodcont.2014.10.010.

Huwe, J.K., Smith, D.J., 2005. Laboratory and on-farm studies on the bioaccumulation and elimination of dioxins from a contaminated mineral supplement fed to dairy cows. J. Agric. Food Chem. 53, 2362–2370. https://doi.org/10.1021/jf0480997.

INRA, Noziere, P., Sauvant, D., Delaby, L., 2018. INRA Feeding System for Ruminants. Wageningen Academic Publishers.

Jandacek, R.J., Tso, P., 2001. Factors affecting the storage and excretion of toxic lipophilic xenobiotics. Lipids 36, 1289–1305. https://doi.org/10.1007/s11745-001-0844-z.

Kelly, B.C., Gobas, F.A., McLachlan, M.S., 2004. Intestinal absorption and biomagnification of organic contaminants in fish, wildlife, and humans. Environ. Toxicol. Chem. 23, 2324–2336. https://doi.org/10.1897/03-545.

Kierkegaard, A., De Wit, C.A., Asplund, L., McLachlan, M.S., Thomas, G.O., Sweetman, A.J., Jones, K.C., 2009. A mass balance of tri-hexabrominated diphenyl ethers in lactating cows. Environ. Sci. Tech. 43, 2602–2607.

Klevenhusen, F., Südekum, K.-H., Breves, G., Kolrep, F., Kietzmann, M., Gerletti, P., Numata, J., Spolders, M., Pieper, R., Kowalczyk, J., 2021. Predicting the transfer of contaminants in ruminants by models: potentials and challenges. ALTEX – Alternatives to Animal Experim. 38, 398–418. https://doi.org/10.14573/altex.2007081.

Kowalczyk, J., Ehlers, S., Oberhausen, A., Tischer, M., Fürst, P., Schafft, H., Lahrssen-Wiederholt, M., 2013. Absorption, distribution, and milk secretion of the perfluoroalkyl acids PFBS, PFHxS, PFOS, and PFOA by dairy cows fed naturally contaminated feed. J. Agric. Food Chem. 61, 2903–2912. https://doi.org/10.1021/jf304680j.

Krause, T., Lamp, J., Knappstein, K., Walte, H.-G., Moenning, J.-L., Molkentin, J., Ober, F., Susenbeth, A., Westreicher-Kristen, E., Schwind, K.-H., Dänicke, S., Fürst, P., Schenkel, H., Pieper, R., Numata, J., 2023a. Experimental study on the transfer of polychlorinated biphenyls (PCBs) and polychlorinated dibenzo-p-dioxins and dibenzofurans (PCDD/Fs) into milk of high-yielding cows during negative and positive energy balance. J. Agric. Food Chem. 71, 13495–13507. https://doi.org/10.1021/acs.jafc.3c02776.

Krause, T., Moenning, J.L., Lamp, J., Maul, R., Schenkel, H., Fürst, P., Pieper, R., Numata, J., 2023b. Transfer of polychlorinated dibenzo-p-dioxins and dibenzofurans (PCDD/Fs) and polychlorinated biphenyls (PCBs) from oral exposure into cow's milk - Part I: State of knowledge and uncertainties. Nutr. Res. Rev. 36, 448–470. https://doi.org/10.1017/s0954422422000178.

Lautz, L.S., Oldenkamp, R., Dorne, J.L., Ragas, A.M.J., 2019. Physiologically based kinetic models for farm animals: Critical review of published models and future perspectives for their use in chemical risk assessment. Toxicol. In Vitro 60, 61–70. https://doi.org/10.1016/j.tiv.2019.05.002.

Lerch, S., Rey-Cadilhac, L., Cariou, R., Faulconnier, Y., Jondreville, C., Roux, D., Dervilly-Pinel, G., Le Bizec, B., Jurjanz, S., Ferlay, A., 2020. Undernutrition combined with dietary mineral oil hastens depuration of stored dioxin and polychlorinated biphenyls in ewes. 2. Tissue distribution, mass balance and body burden. PlosOne. 15, e0230628.

Lerch, S., Siegenthaler, R., Numata, J., Moenning, J.-L., Dohme-Meier, F., Zennegg, M., 2024. Accumulation rate, depuration kinetics, and tissue distribution of polychlorinated dibenzo-p-dioxins and dibenzofurans (PCDD/Fs) in suckler ewes (Ovis aries). J. Agric. Food Chem. 72, 14941–14955. https://doi.org/10.1021/acs.jafc.4c02626.

Lescoat, P., Sauvant, D., Danfær, A., 1996. Quantitative aspects of blood and amino acid flows in cattle. Reprod. Nutr. Dev. 36, 137–174.

Li, M., Gehring, R., Riviere, J.E., Lin, Z., 2018. Probabilistic physiologically based pharmacokinetic model for penicillin g in milk from dairy cows following intramammary or intramuscular administrations. Toxicol. Sci. 164, 85–100. https://doi.org/10.1093/toxsci/kfy067.

Lorenzi, V., Angelone, B., Ferretti, E., Galli, A., Tonoli, M., Donati, M., Fusi, F., Zanardi, G., Ghidini, S., Bertocchi, L., 2020. PCDD/Fs, DL-PCBs, and NDL-PCBs in dairy cows: carryover in milk from a controlled feeding study. J. Agric. Food Chem. 68, 2201–2213. https://doi.org/10.1021/acs.jafc.9b08180.

Mackay, D., 2001. Multimedia Environmental Models: The Fugacity Approach, 2nd ed. CRC Press Taylor & Francis Group, Ann Arbor.

Mackay, D., Shiu WY., Ma KC., Lee SC., 2006. Handbook of Physical-Chemical Properties and Environmental Fate for Organic Chemicals. 2nd ed., Vol II: Haloganated Hydrocarbons. Vol 2nd edition. Ann Arbor: CRC Press Taylor & Francis Group.

MacLachlan, D.J., 2009. Influence of physiological status on residues of lipophilic xenobiotics in livestock. Food Addit. Contam. Part A 26, 692–712. https://doi.org/10.1080/02652030802669170.

MacLachlan, D.J., Bhula, R., 2008. Estimating the residue transfer of pesticides in animal feedstuffs to livestock tissues, milk and eggs: A review. Aust. J. Exp. Agric. 48, 589–598.

Malisch, R., Kotz, A., 2014. Dioxins and PCBs in feed and food — Review from European perspective. Sci. Total Environ. 491–492, 2–10. https://doi.org/10.1016/j.scitotenv.2014.03.022.

Mariman, E.C.M., Wang, P., 2010. Adipocyte extracellular matrix composition., dynamics and role in obesity. Cell. Mol. Life Sci. 67, 1277–1292. https://doi.org/10.1007/s00018-010-0263-4.

Martin, O., Sauvant, D., 2007. Dynamic model of the lactating dairy cow metabolism. Animal 1, 1143–1166. https://doi.org/10.1017/s1751731107000377.

Martin, O., Sauvant, D., 2010a. A teleonomic model describing performance (body, milk and intake) during growth and over repeated reproductive cycles throughout the lifespan of dairy cattle. 1. Trajectories of life function priorities and genetic scaling. Animal 4, 2030–2047. https://doi.org/10.1017/s1751731110001357.

Martin, O., Sauvant, D., 2010b. A teleonomic model describing performance (body, milk and intake) during growth and over repeated reproductive cycles throughout the lifespan of dairy cattle. 2. Voluntary Intake and Energy Partitioning. Animal 4, 2048–2056. https://doi.org/10.1017/s1751731110001369.

McLachlan, M., Richter, W., 1998. Uptake and transfer of PCDD/Fs by cattle fed naturally contaminated feedstuffs and feed contaminated as a result of sewage sludge application. 1. Lactating cows. J. Agric. Food Chem. 46, 1166–1172. https://doi.org/10.1021/jf970922u.

McLachlan, M.S., 1993. Mass balance of polychlorinated-biphenyls and other oraganochlorine compounds in a lactating cow. J. Agric. Food Chem. 41, 474–480. https://doi.org/10.1021/jf00027a024.

McLachlan, M.S., 1994. Model of the fate of hydrophobic contaminants in cows. Environ. Sci. Technol. 28, 2407–2414.

Mikkonen, A.T., Martin, J., Upton, R.N., Moenning, J.-L., Numata, J., Taylor, M.P., Roberts, M.S., Mackenzie, L., 2023. Dynamic exposure and body burden models for per- and polyfluoroalkyl substances (PFAS) enable management of food safety risks in cattle. Environ. Int. 180, 108218. https://doi.org/10.1016/j.envint.2023.108218.

Moenning, J.-L., Lamp, J., Knappstein, K., Molkentin, J., Susenbeth, A., Schwind, K.-H., Dänicke, S., Fürst, P., Schenkel, H., Pieper, R., Krause, T., Numata, J., 2023a. Toxicokinetic modeling of the transfer of polychlorinated biphenyls (PCBs) and polychlorinated dibenzo-p-dioxins and dibenzofurans (PCDD/Fs) into milk of high-

yielding cows during negative and positive energy balance. Comput. Toxicol. 28, 100290. https://doi.org/10.1016/j.comtox.2023.100290.

Moenning, J.L., Krause, T., Lamp, J., Maul, R., Schenkel, H., Fürst, P., Pieper, R., Numata, J., 2023b. Transfer of polychlorinated dibenzo-p-dioxins and dibenzofurans (PCDD/Fs) and polychlorinated biphenyls (PCBs) from oral exposure into cow's milk - part II: Toxicokinetic predictive models for risk assessment. Nutr. Res. Rev. 36, 484–497. https://doi.org/10.1017/s0954422422000208.

Moenning, J.L., Numata, J., Bloch, D., Jahnke, A., Schafft, H., Spolders, M., Lüth, A., Lahrssen-Wiederholt, M., Schulz, K., 2023c. Transfer and toxicokinetic modeling of non-dioxin-like polychlorinated biphenyls (NDL-PCBs) into accidentally exposed dairy cattle and their calves - A case report. Environ. Toxicol. Pharmacol. 99, 104106. https://doi.org/10.1016/j.etap.2023.104106.

Moser, G.A., McLachlan, M.S., 1999. A non-absorbable dietary fat substitute enhances elimination of persistent lipophilic contaminants in humans. Chemosphere 39, 1513–1521.

Reale, E., Jeddi, M.Z., Paini, A., Connolly, A., Duca, R., Cubadda, F., Benfenati, E., Bessems, J., Galea, K.S., Dirven, H., Santonen, T., Koch, H.M., Jones, K., Sams, C., Viegas, S., Kyriaki, M., Campisi, L., David, A., Antignac, J.-P., Hopf, N.B., 2024. Human biomonitoring and toxicokinetics as key building blocks for next generation risk assessment. Environ. Int. 184, 108474. https://doi.org/10.1016/j.envint.2024.108474.

Rey-Cadilhac, L., Cariou, R., Ferlay, A., Jondreville, C., Delavaud, C., Faulconnier, Y., Alcouffe, S., Faure, P., Marchand, P., Le Bizec, B., Jurjanz, S., Lerch, S., 2020. Undernutrition combined with dietary mineral oil hastens depuration of stored dioxin and polychlorinated biphenyls in ewes. 1. Kinetics in blood, adipose tissue and faeces. PlosOne. 15, e0230629.

Richter, W., McLachlan, M.S., 2001. Uptake and transfer of PCDD/Fs by cattle fed naturally contaminated feedstuffs and feed contaminated as a result of sewage sludge application. 2. Nonlactating cows. J. Agric. Food Chem. 49, 5857–5865. https://doi.org/10.1021/jf010859f.

Rosenbaum, R.K., McKone, T.E., Jolliet, O., 2009. CKow: A dynamic model for chemical transfer to meat and milk. Environ. Sci. Tech. 43, 8191–8198. https://doi.org/10.1021/es803644z.

Rozman, K., 1986. Faecal excretion of toxic substances. In: Rozman, K., Hänninen, O. (Eds.), Gastrointestinal Toxicology. Elsevier, Amsterdam/New York/Oxford, pp. 119–145.

Rozman, K., Rozman, T., Greim, H., Nieman, I.J., Smith, G.S., 1982. Use of aliphatic-hydrocarbons in feed to decrease body burdens of lipophilic toxicants in livestock. J. Agric. Food Chem. 30, 98–100. https://doi.org/10.1021/jf00109a022.

Rozman, K., Rozman, T., Smith, G.S., 1984. Liquid paraffins in feed enhance faecal excretion of Mirex and DDE from body stores of lactating goats and cows. Bull. Environ. Contam. Toxicol. 32, 27–36.

Takaki, K., Wade, A.J., Collins, C.D., 2015. Assessment and improvement of biotransfer models to cow's milk and beef used in exposure assessment tools for organic pollutants. Chemosphere 138, 390–397. https://doi.org/10.1016/j.chemosphere.2015.04.032.

Tardiveau, J., LeRoux-Pullen, L., Gehring, R., Touchais, G., Chotard-Soutif, M.P., Mirfendereski, H., Paraud, C., Jacobs, M., Magnier, R., Laurentie, M., Couet, W., Marchand, S., Viel, A., Grégoire, N., 2022. A physiologically based pharmacokinetic (PBPK) model exploring the blood-milk barrier in lactating species - A case study with oxytetracycline administered to dairy cows and goats. Food Chem. Toxicol. 161, 112848. https://doi.org/10.1016/j.fct.2022.112848.

Tedeschi, L.O., 2006. Assessment of the adequacy of mathematical models. Agr. Syst. 89, 225–247. https://doi.org/10.1016/j.agsy.2005.11.004.

Travis, C.C., Arms, A.D., 1988. Bioconcentration of organics in beef, milk, and vegetation. Environ. Sci. Tech. 22, 271–274. https://doi.org/10.1021/es00168a005.

Tremolada, P., Guazzoni, N., Parolini, M., Rossaro, B., Bignazzi, M.M., Binelli, A., 2014. Predicting PCB concentrations in cow milk: Validation of a fugacity model in high-mountain pasture conditions. Sci. Total Environ. 487, 471–480. https://doi.org/10.1016/j.scitotenv.2014.04.042.

Vernon, R.G., 1980. Lipid metabolism in the adipose tissue of ruminant animals. Prog. Lipid Res. 19, 23–106. https://doi.org/10.1016/0163-7827(80)90007-7.

Volpenhein, R.A., Webb, D.R., Jandacek, R.J., 1980. Effect of a nonabsorbable lipid, sucrose polyester, on the absorption of DDT by the rat. J. Toxicol. Environ. Health 6, 679–683.

Weber, R., Herold, C., Hollert, H., Kamphues, J., Blepp, M., Ballschmiter, K., 2018. Reviewing the relevance of dioxin and PCB sources for food from animal origin and the need for their inventory, control and management. Environ. Sci. Eur. 30, 42. https://doi.org/10.1186/s12302-018-0166-9.

WHO, 2010. Harmonization Project Document No. 9 Characterization and Application of Physiologically Based Pharmacokinetic Models in Risk Assessment. World Health Organization Geneva, Switzerland.

Wiener, M., Pittman, K.A., Stein, V.B., 1976. Mirex kinetics in rhesus-monkey. 1. Disposition and excretion. Drug Metab. Disposit. 4, 281–287.

Woodward, A.P., Whittem, T., 2019. Physiologically based modelling of the pharmacokinetics of three beta-lactam antibiotics after intra-mammary administration in dairy cows. J. Vet. Pharmacol. Therap. 42, 693–706. https://doi.org/10.1111/jvp.12812.

Zennegg, M., 2018. Dioxins and PCBs in meat – Still a matter of concern? Chimia 72, 690. https://doi.org/10.2533/chimia.2018.690.